
Article:
Vautrelle, N., Coizet, V., Leriche-Vazquez, M. et al. (8 more authors) (2023) Sensory reinforced corticostriatal plasticity. Current Neuropharmacology, 22 (9). pp. 1513-1527. ISSN 1570-159X

https://doi.org/10.2174/1570159x21666230801110359

Current Neuropharmacology
BENTHAM SCIENCE

Sensory reinforced corticostriatal plasticity

Journal:	*Current Neuropharmacology*
Manuscript ID	CN-2022-0367.R1
Manuscript Type:	Thematic Issue Article
Date Submitted by the Author:	n/a
Complete List of Authors:	Vautrelle, Nicolas; University of Otago, Anatomy Coizet, Veronique ; INSERM, Grenoble Institut of Neuroscience; INSERM Leriche Vázquez, Mariana ; University of Otago, Anatomy Dahan, Lionel; Université de Toulouse, UPS Schulz, Jan; University of Basel, Department of Biomedicine Zhang, Yan-Feng; University of Exeter Medical School, Department of Clinical and Biomedical Sciences Zeghbib, Abdelhafid; The University of Sheffield Overton, Paul; The University of Sheffield, Department of Psychology Bracci, Enrico; The University of Sheffield Redgrave, Peter; The University of Sheffield Reynolds, John; University of Otago, Anatomy
Keywords:	Corticostriatal, plasticity, timing, dopamine, sensory, reinforcement

Sensory reinforced corticostriatal plasticity

Nicolas Vautrelle[1,2†], Véronique Coizet[2,3†], Mariana Leriche[1,2], Lionel Dahan[2,4], Jan M. Schulz[1,5], Yan-Feng Zhang[1,6], Abdelhafid Zeghbib[2], Paul G. Overton[2], Enrico Bracci[2], Peter Redgrave[2] and John N. J. Reynolds[1 *]

[1] Department of Anatomy, Brain Health Research Centre, University of Otago, Dunedin 9054, New Zealand

[2] Department of Psychology, University of Sheffield, Sheffield, S10 2TP, UK

[3] Université Joseph Fourier, Inserm, U1216, Institut des Neurosciences de Grenoble, 38706 La Tronche Cedex, France

[4] Université de Toulouse, UPS, Centre de Recherches sur la Cognition Animale, 118 Route de Narbonne, F-31062 Toulouse Cedex 9, France

[5] Department of Biomedicine, University of Basel, CH - 4056 Basel, Switzerland

[6] Department of Clinical and Biomedical Sciences, University of Exeter Medical School, Hatherly Laboratories, Exeter EX4 4PS, United Kingdom

[†] These authors contributed equally to this work

[*] To whom correspondence should be addressed.

E-mail: john.reynolds@otago.ac.nz

Phone : +64 3 4795781

One sentence summary: A novel form of *in vivo* corticostriatal plasticity is reported where striatal spiking evoked by single pulse stimulation of motor cortex was potentiated by a natural sensory reinforcer, operating via intact afferent projections, with behaviorally relevant timing.

Abstract

Background: Regional changes in corticostriatal transmission induced by phasic dopaminergic signals are an essential feature of the neural network responsible for instrumental reinforcement that occurs during action discovery. However, the timing of signals in early models of corticostriatal plasticity is difficult to reconcile with behavioral reinforcement learning where the reinforcer is normally delayed with respect to the selection and execution of causally-related actions.

Objective: While recent studies have started to address the relevance of delayed reinforcement signals and their impact on corticostriatal processing, our objective was to establish a model in which a sensory reinforcer triggers appropriately delayed reinforcement signals relayed to the striatum via intact neuronal pathways and to investigate the effects on corticostriatal plasticity.

Methods: We measured corticostriatal plasticity with electrophysiological recordings, a light flash as a natural sensory reinforcer, and pharmacological manipulations in an *in vivo* anaesthetized rat preparation.

Results: We demonstrate that the spiking of striatal neurons evoked by single pulse stimulation of motor cortex can be potentiated by a natural sensory reinforcer, operating through intact afferent pathways, with signal timing approximating that required for behavioral reinforcement. The observed potentiation of corticostriatal neurotransmission was attenuated by pharmacological blockade of dopamine receptors.

Conclusion: This novel *in vivo* model of corticostriatal plasticity offers a behaviorally relevant framework with which to address the physiological, anatomical, cellular and molecular bases of instrumental reinforcement learning.

Keywords: Corticostriatal, plasticity, timing, dopamine, sensory, reinforcement

Graphical abstract:

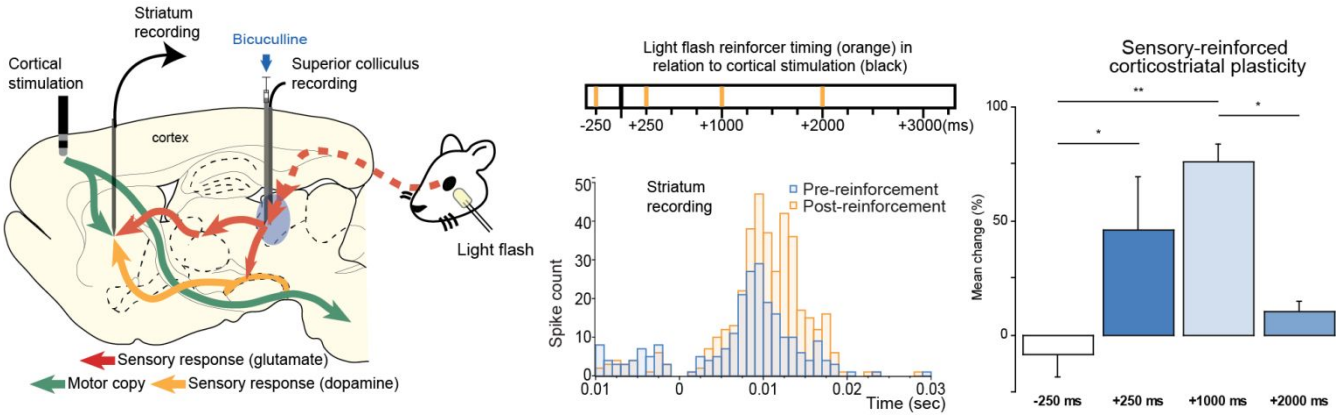

1. Introduction

A century ago, Thorndike's cat was confined in a cage until, unwittingly, it pressed against a pedal which opened the cage-door, giving the animal access to a piece of fish [1]. With repeated trials, the animal gradually learned what it had to do, so, when placed in the cage again, it was able to select the newly acquired action of pedal pressing and gain immediate access to the fish. This first formal demonstration of instrumental conditioning exemplifies reinforcement-driven action acquisition where an unexpected sensory reinforcer (the cage-door opening) enables relevant neural systems to converge onto the causal aspects of the cat's behaviour, the pedal press. Accumulating empirical evidence points to the basal ganglia, specifically the dorsal striatum, playing a critical role in such reinforcement-driven action acquisition [2-6]. In most models of this process [7-10], signals assumed to represent behavioural options originating from the cerebral cortex induce patterns of activity in the striatum, which are differentially reinforced by consequent sensory events that evoke phasic signals from midbrain dopaminergic neurons. Phasic dopamine (DA) activity is evoked by unexpected, non-habituated sensory events [11-14], including those associated with reward [14-17]. Historically, two central experimental protocols have been used to investigate the biological mechanisms of corticostriatal plasticity: (i) high-frequency stimulation of afferent corticostriatal fibres in association with postsynaptic neuron firing [18]; and (ii) spike-timing-dependent-plasticity (STDP) protocols in which pre- and post-synaptic activity in striatal neurons is manipulated to demonstrate long-term changes in corticostriatal transmission [19-22]. These paradigms have shown that the timing of activation of the pre- and post-synaptic elements and the presence/absence of DA are critical for certain forms of corticostriatal plasticity [17, 18, 21, 22]. It has, however, been difficult to reconcile the timing aspects of early experimental protocols with behavioural reinforcement in which delayed reinforcing sensory signals (the cage door opening in the case of Thorndike's cat), typically occur hundreds of milliseconds, sometimes seconds, after the relevant causal behaviour (the cat pushing the pedal) [23-26]. Many studies over the past decades have investigated the impact phasic dopaminergic signals have on corticostriatal processing underlying action selection during the execution of well-learned tasks [27-32]. However, studies that have investigated the relative timing of afferent cortical and dopaminergic signals on lasting corticostriatal plasticity underlying action discovery are limited. For example, the timing of dopaminergic signals seems to be crucial for modulating the structural plasticity of dendritic spines of medium spiny neurons (MSN) [33], the STDP of corticostriatal synapses on D1 and D2-type receptor-expressing MSN [34-36], and the interaction with cholinergic signalling in the induction of short-term corticostriatal potentiation [37]. However, a model of lasting corticostriatal plasticity in which the temporal dynamic of signals likely to converge within the striatum can be systematically manipulated at timescales

consistent with action discovery, remains to be interrogated. To address this issue our strategy was to develop an in vivo preparation that permitted precise control over afferent signalling within the relevant neural network.

Based on our analysis of basal ganglia functional anatomy [5, 6] and in accordance with the neoHebbian three-factor learning rules [24, 25, 38], we sought to model three principal sources of input likely to be engaged during natural visually reinforced instrumental conditioning (Fig. 1A): (i) the afferent collateral fibres, branching from motor cortical projections to the brainstem, which ensure that the striatum receives a running copy of the motor commands directing behavioural output [39, 40]; (ii) the short-latency information signalling the occurrence of an unexpected, salient visual event, relayed via ascending glutamatergic thalamostriatal projections [40-43]; and (iii) the short-latency, visually-evoked, phasic DA input from substantia nigra [44], widely considered to act as a critical reinforcement signal for corticostriatal plasticity [15, 17]. Following the onset of a potentially reinforcing salient visual event, an important source of short-latency input to both nigral DA neurons and thalamic regions that project to the striatum, is from branching tecto-nigral/tecto-thalamic fibres that originate from deep layer neurons of the midbrain superior colliculus (Fig. 1A) [45-47]. Earlier studies by our group have demonstrated that these bifurcating projections will ensure that a single reinforcing visual event can evoke near-simultaneous, and potentially converging phasic inputs of DA and glutamate (GLU) into the striatum [43, 44]. Coincident DA and GLU input to the striatum has been shown to be essential for the activation of the plasticity marker ERK and the expression of drug-induced locomotor sensitization [48]. With this point in mind, we exploited our knowledge of how to use a neutral stimulus (a light flash) repetitively to produce combined short-latency, visually-evoked release of DA [44] and GLU [43] into the striatum via intact pathways in anaesthetized rats (Fig. 1A). These procedures rely on the important discovery of Katsuta et al. [49] who showed that a local injection of the GABAA antagonist bicuculline into the superior colliculus can restore visual responsiveness to deep layer neurons, previously rendered insensitive by anaesthesia. Therefore, the present study was designed to: i) test whether sensory-reinforced corticostriatal plasticity could be demonstrated by pairing electrical stimulation of motor cortex with simultaneous and appropriately timed sensory-evoked inputs from the thalamus (GLU) [43] and substantia nigra (DA) [44]; ii) test whether the temporal dynamics of the observed sensory-reinforced plasticity conformed to the timing of behavioural reinforcement learning; and iii) determine the extent to which intact dopaminergic neurotransmission is essential for this form of corticostriatal plasticity. In our model, the precisely controlled electrically evoked input from the motor cortex takes the place of a motor command (e.g. a pedal press), which could be causally related to a consequent light flash, (in the case of Thorndike's cat, the door opening). Our prediction was that appropriate timing of the cortical-motor and visually-evoked sensory inputs should induce

prolonged reinforcement of the corticostriatal response in this potentially causal association [5, 10]. The demonstration of a novel, behaviourally relevant, in vivo model of sensory reinforced corticostriatal plasticity confirmed this prediction. Subsequent experiments showed that the observed potentiation of corticostriatal transmission was partially suppressed by a pharmacological blockade of dopamine receptors.

2. Materials and Methods

2.1 Care of animals: All animal husbandry and experimental procedures were performed in the UK with Govt. Home Office approval under section 5(4) of the Animals (Scientific Procedures) Act 1986. In New Zealand, experiments were conducted in compliance with the Animal Welfare Act 1999. Experimental protocols also received prior approval of the relevant Institutional Ethics Committees.

2.2 Surgical techniques: Seventy-six Hooded Lister and 9 Long Evans male rats (250-450 g) were prepared for electrophysiological recording under urethane anesthesia (1.25-2.0 g/kg). A concentric bipolar stimulating electrode (NEX-100, Rhodes Medical Instruments, Inc.) was introduced in the primary motor cortex (AP +3.7 to +2.2 mm, bregma; ML +2.0 to +3.0 mm, midline; DV -1.3 to -2.0 mm, dura). A tungsten microelectrode (A-M Systems, Inc., 2 MΩ) glued to a 30-gauge metallic injector needle filled with bicuculline methiodide (Sigma Aldrich, 100 ng/µl 0.9% saline) was placed vertically into the intermediate layers of the ipsilateral lateral superior colliculus (AP -6.3 to -7.3 mm, bregma; ML + 1.5 to 2.5 mm, midline; DV -4.5 to -5.3 mm, dura). An ipsilateral approach (angled 15° in the medio-lateral plane; AP +0.2 to -0.8 mm, bregma; ML +2.0 to +3.5 mm, midline; DV -5.0 to -6.0 mm, dura) was used to position a multi-unit (2 MΩ tungsten or NeuroNexus, 16 channels) or single-unit microelectrode (6-13 MΩ glass pipette, internal solution: 0.5M potassium acetate) into the striatal receptive field responsive to motor cortical stimulation ([40, 50] and Fig. S1). In the experiments where striatal microinjections of lidocaine (20-40 nl, 40 µg/µl, Sigma Aldrich) were made, a 30 µm diameter glass injection pipette was glued to the striatal single channel tungsten microelectrode.

2.3 Recording techniques: A Micro 1401 hardware acquisition system connected to a standard PC running Spike 2 software (Cambridge Electronic Design) was used to sample striatal and collicular local field potential (filter setting: DC-50 Hz) and multi- or single-unit activity (filter setting: 0.2-15 kHz, sampling rate: 15 kHz). A System 3 modular rack-mount workstation (Tucker-Davis Technology) connected via a F15 Gigabit interface to a

standard PC running a custom Matlab™ script was used to sample striatal 16 channels multiunit activity (unfiltered signal, sampling rate: 25 kHz).

In the first series of experiments (Figs. 1B and 2), multi-unit responses to ipsilateral motor cortex stimulation (single 100 µs duration pulse, 0.2-1.0 mA intensity, single pulse recurrence 0.5 Hz, 30% jittered) were recorded in the striatum and the superior colliculus. After recording 6 blocks of cortical stimulation-evoked responses (120 stimulations/block), each motor cortex stimulation was paired with a whole-field light flash (10ms duration) delayed by +250ms. The flash was delivered from a green LED (570 nm, 60 LUX) positioned 5 mm from the eye contralateral to the stimulation and recording electrodes. After recording 6 more stimulation blocks (120 stimulations/block), bicuculline methiodide was injected into the lateral deep layers of the superior colliculus (0.5 µl, 1 µl/min). Disinhibition of the superior colliculus, assessed by online observation of a clear multi-unit response evoked by the light flash, typically lasted 10-20 min. When the disinhibitory effect of bicuculline had worn off, the light flash was discontinued. Recording of striatal and collicular responses to motor cortex stimulation continued for up to 3 h.

In the second set of experiments (Figs. 1C and 3), the ipsilateral single pulse cortical stimulation was delivered with a 0.2 Hz recurrence, in order to accommodate our longer reinforcement delay of +2 sec. After recording 3 blocks of cortical stimulation-evoked responses (120 stimulations/block), each motor cortex stimulation was paired with a light flash presented either before (-250 ms, N=7) or after (+250 ms, N=4; +1000ms, N=4; or +2000 ms, N=4) the cortical stimulation pulse. After recording 3 more stimulation blocks, bicuculline methiodide was injected in the lateral deep layers of the superior colliculus (0.5 µl, 1 µl/min). Following the disinhibitory effect of bicuculline, the light was switched off and striatal and collicular responses to motor cortex stimulation were recorded, again for up to 3 h.

In the third series of experiments (Figs. 1D and 6), multi-unit responses to ipsilateral motor cortex stimulation (0.33 Hz recurrence) were recorded in the striatum over 16 channels (Fig. S1B). After recording 4 blocks of cortical stimulation-evoked responses (120 stimulations/block), the animals received an i.p. injection of either saline (0.9%), D1-type dopamine receptor antagonist SCH 23390 hydrochloride (0.2 mg/kg, Sigma), D2-type dopamine receptor antagonist Sulpiride (30 mg/kg, Sigma) or both D1 and D2-type dopamine receptor antagonists. After recording 4 more stimulation blocks (24 mins), each motor cortex stimulation was paired with a light flash presented 250 ms after the cortical stimulation pulse. After recording 4 more blocks, bicuculline methiodide was injected in the lateral deep layers of the superior colliculus (0.5 µl, 1 µl/min). Following the

disinhibitory effect of bicuculline, the light was switched off and striatal and collicular responses to motor cortex stimulation were recorded, again for up to 3 h.

During single-unit recording experiments (see Fig. 4), single pulse cortical stimulation of the motor cortex was delivered with a 0.2 Hz recurrence (0.5-1 mA, 0.1 to 0.25ms) and paired with a light flash delayed by +250ms. After recording one block of cortical stimulation-evoked responses (60 stimulations/block) and one block of cortical stimuli paired with the light flash, bicuculline methiodide (0.2-0.3 µl, 0.4 µl/min) was injected in the lateral superior colliculus. Visual stimulation continued until the collicular disinhibition was no longer present. Recording of the response of striatal neuron to motor cortex stimulation was maintained until the cell was lost (30-90 min). In some single unit experiments, the stimulating electrode was placed in the contralateral motor cortex (AP 2.0 mm bregma; ML -1.6 mm midline; DV -2.3 mm, dura). The pattern of response plasticity was similar to that obtained using ipsilateral electrode placements, hence these experiments were considered together.

2.4 Histology: Following the experiment, animals were perfused intracardially with saline (0.9%) followed by paraformaldehyde (4%) and their brains taken for histological analysis. Using standard immunohistochemical procedures, sections of cortical, striatal and collicular tissues were reacted to reveal Fos-like immunoreactivity (rabbit polyclonal antibody, 1:20,000 dilution) evoked by electrical, sensory and chemical stimulation. Fos-like immunoreactivity was only detected in the superior colliculus of animals that had received a bicuculline injection. The distribution of Fos-positive neurons was subjectively analysed to determine the extent of the collicular area activated by each bicuculline injection (see Fig. S2C). Other sections were stained with cresyl-violet to verify the locations of the recording and stimulation sites (Figs. S2, S3 and S4).

2.5 Data analysis: Data were processed off-line using CED Spike 2 and Matlab™ software and custom scripts. Multi-unit activity was extracted from high-pass filtered waveforms by applying a threshold determined over the baseline recordings for each experiment to include a wide range of striatal neurons responsive to motor cortex stimulation (Fig. 5). For both multi- and single-unit recordings, spike-count rasters and peri-stimulus time histograms were aligned on cortical stimulation onset (Figs. 5B and S7A). For the first 2 series of experiments, a threshold value (mean frequency + three times the standard deviation of the mean frequency) was calculated over 500 ms of baseline spontaneous activity preceding the cortical stimulation (Fig. 5C). The peak of the cortically-evoked response was then detected during the 50 ms following stimulation. The evoked-response onset and offset were defined as the time of the first bin to exceed or fall below the threshold before and after the peak, respectively. Response magnitude was defined as the number of spike counts during the evoked response, minus the mean

baseline count for the same period (Fig. 5C green). The value for each block (120 cortical stimulations) was normalized for each subject as a percentage change relative to the mean value of the blocks obtained prior to the injection of bicuculline. For the third set of experiments, striatal responses to cortical stimulation were obtained by subtracting from each peri-stimulus time histogram its own mean spontaneous firing calculated over the 500 ms of spontaneous activity preceding the cortical stimulation (Fig. S7A – green line). An average baseline response to cortical stimulation was then calculated for each channel over the 8 blocks preceding the bicuculline injection (4 post-drug blocks of stimulation + 4 post-drug blocks of stimulation paired with light flash; Fig. S7C blue period and Fig. S7B blue traces). Over all channels, peaks of potentiation were then detected for each block. A peak of potentiation was detected (Fig. S7B red dots) if a bin value in the block response (Fig. S7B green trace) was greater than the sum of the same bin value in the average baseline response (Fig. S7B blue trace) plus two standard deviations (Fig. S7B blue shading). Potentiation peaks were then plotted against time over the experiment (Fig. S7C). A channel was considered potentiated if it met one of the following requirements: i. following bicuculline injection, potentiation peaks with similar latencies were detected over a minimum of 5 consecutive blocks and such peaks were absent during the pre-drug period; or ii. following bicuclline injection, potentiation peaks with similar latencies were detected over seven or more consecutive blocks and such peaks were absent during the pre-drug period.

The latency of the potentiated response was defined as the time between the electrical stimulation and the first bin of the potentiated response. The duration of the potentiated response was defined as the number of bins over which a potentiated response was observed. To determine the magnitude of potentiation, the spike-count values for each peak of potentiation were calculated as the difference between the bin value of the block response (green trace) and the bin value of the average baseline response (blue trace). The total magnitude of the potentiation of the response was then calculated by summing the spike counts of all peaks of potentiation. The average magnitude of the potentiation was calculated by dividing that sum by the duration of the potentiated response.

2.6 Statistical analysis: Group comparison of cortical stimulation-induced striatal responses elicited over the full time period were made using a repeated measures ANOVA to separate group and time effects. A Mann Whitney U test was used to compare over all experimental conditions the non-normally distributed mean change (%) in striatal response magnitude data at 44-56 min after collicular disinhibition. Changes from baseline were assessed using a Wilcoxon matched-pairs-signed-rank and Kruskal-Wallis tests. Within-group effects were analysed using paired t-tests.

To assess the effect of the dopamine antagonist(s) on striatal responses to cortical stimulation (Pre-drug baseline period (purple) vs Post-drug baseline period (blue) in Fig. S7C), an ANOVA-like table with tests of random-effect terms (RANOVA) was used [51]. This statistic is employed as a measure of the size of the difference between the conditions. To determine the effect of the drug treatments on the proportion of electrode channels on which pairing induced significant potentiation, a Chi-Square test was used. Significance was considered for two-tailed P values < 0.05.

3. Results

To simulate motor-copy input to the striatum in a controlled manner, single electrical pulses (0.1 ms; 0.2-1.0 mA; 0.5 Hz) were delivered to the ipsilateral motor cortex (Figs. S2A, S3A and S4A) and recordings made from neurons in the dorsal striatum (Figs. S2B, S3B and S4B). Sensory reinforcement was provided by a contralateral whole-field light flash in the presence of a disinhibitory injection of bicuculline (50 ng/ 500nl), into the deep layers of the superior colliculus [49] (Figs. S2C, S3C and S4C). We have shown this treatment ensures that each light flash can effectively activate nigral and thalamic input to the striatum over an extended period [43, 44]. Thus, each cortical pulse was followed by a reinforcing light flash with a delay of 250ms (Fig. 1B). This value was chosen on the basis of behavioural delayed reinforcement data [23]. At the outset we were unsure which, if any, striatal neurons would be affected by this paradigm. We therefore thought it prudent to record a multi-unit response (Fig. 2) to the cortical electrical stimulus within the motor territories of the striatum (Figs. S1A, S2B, S3B and S4B).

3.1 Converging afferent signals are required for corticostriatal potentiation: As predicted from previous work [43, 44, 52], the suppressive effects of urethane anaesthesia on visual sensory responding in the collicular deep layers also blocked all sensory reinforcement of cortically-evoked striatal activity (all visually-reinforced trials preceding time-0 in Fig. 2A). However, following disinhibitory injections of bicuculline into the superior colliculus, local collicular neurons became visually responsive (Fig. 2C: top), facilitating the relay of sensory signals to the striatum via the tecto-nigro-striatal and tecto-thalamo-striatal projections [43, 44]. Although collicular disinhibition enabled the light flashes to induce reliable visually-evoked local field potentials in the striatal territory receiving input from the motor cortex (Fig. 2C: middle), flash-induced spiking in this part of the striatum was rarely observed (Fig. 2C: bottom). In contrast, multi-unit responses in the striatum evoked by continuing motor cortex single pulse stimulation were progressively enhanced by the visual reinforcer (Fig. 2A

blue line and Fig. 2B; repeated-measures ANOVA of group data, condition x time interaction, $F_{12,84} = 3.6$; $P = 0.0002$). This potentiation of corticostriatal transmission lasted for at least 1 h after the local disinhibitory effect of bicuculline had worn off – indicated by collicular neurons becoming unresponsive again to the visual stimulus. Representative examples of the facilitation of striatal multi-unit spiking activity caused by visual reinforcement are illustrated in Figs. 2B and S5A-E. Comparable potentiation of corticostriatal transmission was not observed when either the light-flashes (Fig. 2A: green line) or the disinhibitory injections of bicuculline (Fig. 2A: red line) were omitted from the protocol. These control conditions confirmed first, that visually-triggered reinforcing inputs to the striatum cannot occur in the absence of signalling from the deep layer of the superior colliculus; and second, that the potentiation observed depends on the precisely timed visual stimulation as any non-specific activation caused by the general disinhibitory effects of intracollicular bicuculline were ineffective (cortical stimulation + collicular bicuculline – green line in Fig 2A).

Further, to test the possibility that bicuculline-gated sensory reinforcement was having a general sensitizing effect in the striatum, unrelated to the electrically-evoked corticostriatal input, the electrical stimulation of motor cortex was turned off during the period of sensory reinforcement. When the SC had stopped responding to the light flash, the cortical stimulation was reinstated. Potentiation of the striatal response was then significantly attenuated (Fig. 2D: blue vs yellow bars; Mann Whitney, $U = 3$, $P < 0.02$). Thus, a timed co-activation of cortical and sensory inputs was necessary for a full expression of sensory-reinforced potentiation of corticostriatal transmission.

However, due to the re-entrant looped architecture of the cortico-basal ganglia projections [53, 54], it is still difficult to ascertain the locus of plasticity *in vivo*. To exclude the possibility that sensory reinforcement was acting independently of transmission through the striatum, a further control experiment was conducted in which tissue surrounding the striatal recording electrode was temporarily inactivated by a local injection of the topical anaesthetic lidocaine during the period of sensory reinforcement. When cortically-evoked spiking in the striatum recovered from the local anaesthetic, the striatal response to cortical input was significantly depressed (Fig. 2D: blue vs purple bars; Mann Whitney, $U = 0$, $P < 0.005$). This attenuation was not due to a lack of recovery or to a possible mechanical damage induced by the local injection of lidocaine as striatal spontaneous spiking after dissipation of the lidocaine effect was similar to that observed before injection (average baseline frequency count before lidocaine 31.7 ± 2.9 Hz vs 29.1 ±2.8 Hz after lidocaine; paired t-test, $P > 0.1$), while cortically-evoked response magnitude was reduced (before lidocaine 1.97 ± 0.13 vs 1.28 ± 0.19 after lidocaine; paired t-test, $P < 0.002$). Subsequent analyses were conducted on data from each condition where the mean post-treatment

magnitude of the striatal response (+44 to +56 min – the grey shaded area in Fig. 2A) was compared with relevant data from the baseline period preceding treatment (-48 to 0 min). A reliable change from baseline was observed only when cortical stimuli were reinforced with light flashes presented during the period of collicular disinhibition (Wilcoxon matched-pairs-signed-rank test $Z = -2.366$; $P = 0.018$). This increase in amplitude of the cortically-evoked response was accompanied by a significant increase in its duration (Fig. S6B, Kruskal-Wallis, $H = 26$, d.f. $= 4$, $P < 0.0001$) while its latency was unchanged (Fig. S6A, Kruskal-Wallis, $H = 4.5$, d.f. $= 4$, $P = 0.35$). Together, the control experiments showed that the convergence within the striatum of cortical and sensory-evoked reinforcing inputs was a necessary requirement for corticostriatal potentiation to be observed.

3.2 Appropriate signal timing required: A critical feature of behavioural reinforcement is that when a reinforcer precedes or is delayed too long after a causal action, its reinforcing effect is greatly diminished [23, 26, 38]. Consequently, to see if these principles also apply in the current model of corticostriatal plasticity, sensory reinforcement was presented at different times relative to the input to the striatum from motor cortex. To accommodate an increased delay of the sensory reinforcement in this part of the study, the frequency of the cortical stimulation was reduced to 0.2 Hz (Fig. 1C). Under these conditions and consistent with behavioural studies, significant potentiation was observed only when sensory reinforcement occurred within a limited temporal window (+250 and +1000ms) following the signal from the motor cortex (Figs. 3 and S5G and H). Sensory stimuli presented before (-250ms) or too long (2000ms) after cortical stimulation were comparatively ineffective. Moreover, in accordance with the reduced number of reinforcement pairings presented during the period of collicular disinhibition in this protocol (recurrence of pairing 0.2 vs 0.5 Hz), the magnitude of the potentiation effect was also significantly reduced (c.f. Figs. 2D and 3, for the +250 ms condition only; Mann Whitney, $U = 10$, $P < 0.04$).

3.3 Potentiation of single-unit activity: Next, we sought to explore ways in which the observed enhancement of the multi-unit response may be understood in terms of the effect of sensory reinforcement on the responses of single striatal units. When single pulse cortical stimulation (0.2 Hz) was coupled to sensory reinforcement (light-flashes delivered +250ms after the cortical stimulus) in the presence of collicular disinhibition, potentiation was observed in 8/11 recordings from single striatal neurons. From these data, the gradual increase in potentiation seen in the multi-unit response (Fig. 2A) could be understood, in part, by the variable delays in the onset of the potentiation expressed by individual neurons (Fig. 4A). Secondly, the potentiation of multi-unit spiking (Fig. 2) was likely to reflect some neurons increasing their probability of firing at the same specific latencies at which

they fired before potentiation (e.g. green neuron in Fig. 4). Alternatively, other neurons would start responding to the cortical stimulation at new latencies, while at the same time maintaining similar spiking probabilities at pre-potentiation latencies (blue neuron in Fig. 4). Presumably, this variable pattern of firing latencies expressed by individual striatal neurons (Figs. 4B & C and S5F) reflects a combination of distinct afferent corticostriatal and intrastriatal contacts. The short latency evoked striatal responses (<12 ms) are most likely to be driven by monosynaptic cortical inputs [55], while the longer latency components (>12 ms) probably reflect multisynaptic contacts. Interestingly, sensory reinforcement seems capable of modulating both mono- and multisynaptic inputs [35]. This, in part, would explain the overall pattern of potentiation we observed in our multi-unit recordings.

3.4 Multiple sources of plasticity: Appropriately timed phasic dopaminergic neurotransmission is considered an essential factor for the induction of corticostriatal plasticity [18, 21, 34]. To test this we conducted our plasticity protocol in the presence of systemically administered D1-type (SCH23390) and D2-type (sulpiride) dopamine receptor antagonists. In preparation for interpreting the effects of dopamine antagonists before and after the induction of plasticity, in these experiments we used vertically aligned 16-channel electrodes to record cortically evoked multi-unit activity within a larger area of striatal tissue (Figs. S1B and S4B). Because the channels extend 1.5 mm above the tip at a 10° angle, the recording sites of these 16 channel electrodes are more ventrolateral than suggested by the tip location, and are likely sampling from a similar area to the other two experiments. After recording a pre-drug baseline control period (Fig. S7C), each subject was injected IP with either 1ml/kg of saline (0.9%; N=4), the D1 dopamine receptor antagonist SCH23390 (0.2mg/kg; N=5), the D2 dopamine receptor antagonist sulpiride (30 mg/kg; N=5), or an injection that contained both dopamine receptor blockers at the same respective concentrations (N=5). A post-drug baseline period was then recorded, part of which included light reinforcement in the absence of collicular disinhibition (Fig. S7C).

To determine the effects of DA antagonists on baseline striatal responding [56] and to detect the subsequent presence of a potentiated response on single recording channels, we constructed post-stimulus time histograms for successive blocks of 120 cortical stimulations (Fig. S7A). When comparing the initial and drug baseline periods (blocks 1-4 v.s. blocks 5-12 in Fig. S7C) we confirmed that the D1-type receptor antagonist reliably suppressed the striatal response to cortical stimulation ($F=28.55$, $P = 0.0001$, using a randomisation test based on the F statistic [51]), while the striatal response was enhanced by the D2-type receptor blocker ($F=4.81$, $P = 0.0321$ [51]; Fig. S8). When the DA antagonists were administered in combination, there was a small but reliable increase in baseline striatal responses ($F=9.71$, $P = 0.0015$ [51]; Fig. S8). Finally, there were no reliable differences

between the effects of dopamine antagonists on the baseline responses recorded on the electrode channels that would later potentiate, compared with those that did not (Fig. S8).

Since we were now sampling from multiple sites in the striatum, the next step was to determine for each animal on how many of the multielectrode's 16 channels could the cortically evoked neural response be detected. Typically, several adjacent channels were responsive, thereby confirming the restricted patterns of striatal responsiveness observed when moving a single electrode (c.f. Figs. S4A and S4B). Consistent with previous experiments, evoked responses comprised time-locked increases in spiking that resolved into peaks of activity at fixed latencies (Figs. S7A and S7B).

We then analysed the results from animals in which the two DA receptor blockers were separately administered by comparing the histograms of blocks following sensory-reinforcement with the average histogram from a post-drug-baseline period (Fig. S7B and S7C). The main finding was that, compared with the saline control group, either DA receptor blocker significantly reduced the proportion of electrode channels on which potentiation was recorded (Fig. 6; D1-type antagonist – Chi-Square 11.5, df = 1, $P < 0.001$; D2-type antagonist – Chi-Square = 15.9, df = 1, $P < 0.001$). However, on channels where it remained, the observed potentiation was largely unaffected by the DA antagonists; i.e. the mean duration, latency and magnitude of the potentiation was not statistically different from the values obtained from the saline control group. Lastly, we determined the effects of a combined blockade of D1-type and D2-type dopamine receptors on the corticostriatal plasticity induced by sensory reinforcement. Compared with the saline control group, response potentiation was again observed on significantly fewer electrode channels (Chi-Square 11.6; df=1; $P = 0.001$; Fig 6). However, the overall duration, magnitude, and latencies, of positive instances of potentiation were again not reliably different from the saline control condition. We therefore conclude that blocking D1-type and D2-type receptors effectively reduced, but did not abolish, the number of spatially distributed channels in the striatum on which sensory-reinforced potentiation could be observed.

4. Discussion

The present study established an *in vivo* model of corticostriatal plasticity by which to explore the effects of delayed reinforcement signals generated by a natural sensory stimulus [13] and relayed into the striatum via intact afferent projections [43, 44, 46]. Validation of this protocol as an *in vivo* model of corticostriatal plasticity was

strengthened after plasticity on behavioural time scales was observed. The main result of the study was that multi-unit striatal responses evoked by electrical stimulation of the motor cortex were potentiated by a delayed light flash under experimental conditions known to promote visual sensory input to the striatum [43, 44]. The magnitude of the observed potentiation was quantitatively related to the number of stimulation-reinforcement pairings. Importantly, the observed potentiation of corticostriatal transmission was maximised when a behaviourally relevant time delay was imposed between input from the motor cortex and the sensory reinforcement. Reinforcement administered prior to, or too long after the cortical input was ineffective. Therefore, this model of sensory-induced corticostriatal plasticity shares important aspects with the reinforcement that happens during behavioural conditioning [1, 23]. In both cases, an unexpected sensory event that occurs prior to a particular behavioural output cannot have been caused by the latter, therefore the process of reinforcement should not operate. Similarly, an excessive delay between an action and a consequent reinforcing event invokes an increasingly difficult credit assignment problem, especially if irrelevant actions are expressed during the delay period. Thus, in both our model and behavioural conditioning, effective reinforcement only occurs if a potentially contingent sensory reinforcer arrives several hundreds of milliseconds after the neural representation of a causal motor output. This result therefore supports neoHebbian three-factor learning rules and corroborates the idea that motor-related input to the striatum generates a decaying synaptic eligibility trace that establishes a critical time window within which reinforcement must occur to induce potentiation [24-26, 38]. A mechanistic instantiation of this idea is provided by recent studies that have investigated the impact of delayed dopamine release on Hebbian plasticity at the corticostriatal synapse [33, 34, 36]. For example, in D1-type receptor expressing medium spiny neurons, Yagishita et al. [33] showed that structural plasticity of dendritic spines was dependent on the sequential activation of the NMDA-receptor and dopamine D1-type receptor signalling pathways within a similarly restricted time window. Likewise, the potentiation of positive corticostriatal STDP by a delayed reinforcer in D1-type and D2-type receptors expressing striatal neurons was not observed if the activation of the dopamine inputs to the striatum [34] or the uncaging of dopamine [36] occurred with delays greater than ~2s after the corticostriatal pairing. The current protocol therefore offers a novel *in vivo* paradigm with which to evaluate the physiological, cellular and molecular mechanisms underlying the concept of reinforcement-eligibility [17].

The results show that the reinforcing effect of visual stimuli in the present study, under conditions where phasic DA is known to be released [44], occurred at subthreshold levels and in the absence of any changes in striatal spiking activity (Fig. 2C). This could provide important insights into the mechanisms of sensory reinforcement during behavioural instrumental conditioning [57, 58]. However, to understand how this might be the case it is

necessary to appreciate that instrumental reinforcement operates to bias the selection of future actions (i.e. modulates the frequency with which reinforced actions are selected). Therefore, it is to be expected that the mechanism(s) underlying behavioural reinforcement would be present within the neural systems responsible for action selection [5, 8, 57-59]. A recurring theme within basal ganglia research is that they constitute a mechanism within the vertebrate brain for selecting between competing behavioural motivations and actions [60-62]. The proposed mechanism of selection is by selective disinhibition [63] within the parallel loop architecture of the basal ganglia [64, 65]. Instrumental reinforcement is thought to potentiate transmission in recently eligible (selected) channels, thereby increasing their probability of future re-selection [5, 57, 58, 66]. Insofar as 'recently active channels' cannot be predicted, reinforcement signals would need to be broadcast widely across the competing channels. It is therefore relevant that afferent projections likely to carry short-latency signals reporting the occurrence of an unpredicted sensory reinforcer (both nigro-striatal DA and thalamo-striatal GLU), project widely throughout the striatum [40, 67-69]. Within such an architecture, it is interesting to note in the current model of corticostriatal plasticity that sub-threshold reinforcer-driven depolarization [35, 43, 70] (see also Fig. 2C), rather than an induction of all-out spiking, is preferred to adjust the sensitivity of recently active channels [66].

How sensory reinforcement might operate on the multiple cell-types and synaptic connections within the striatal microarchitecture will inevitably be complicated. The current *in vivo* model of cortico-striatal plasticity has revealed a complexity and diversity of potential synaptic changes. From our single-unit recordings of putative medium spiny neurons (MSNs), the observation that sensory reinforcement can potentiate existing responses (Fig 4C green trace) and induce spiking at previously unresponsive latencies (Fig 4C blue trace) suggests the reinforcement process can operate at multiple synaptic locations and possibly across multi-synaptic pathways. This idea is reinforced by the finding that potentiated responses to cortical stimulation can occur at short latency (< 12 ms), but also at much longer latencies (up to 20 – 25 ms, Fig 4C, S5 and S7C). Potentiation observed in our multi-unit responses could result from changes in intrinsic excitability of MSNs, dependent on D1-type receptors and A2a-receptor signalling [22, 34], but also from changes in synaptic transmission at glutamatergic synapses formed on MSNs [71, 72] and on striatal interneurons [73, 74]. While the identification of the different striatal cell-types was not the remit of the current test of whether any plasticity was detectable, a principle has been established where future studies using spike sorting from multichannel electrode arrays [75-77] can interrogate how sensory reinforcement can independently modulate components of intrinsic striatal microcircuitry. Further, our results show that the point at which cortico-striatal potentiation can be observed following a period of sensory-reinforcement is highly variable. Thus, some of the observed potentiation occurred soon after the reinforcement

period had commenced, yet in other cases it became evident only 40 to 60 min after its cessation (Fig 4). This is further evidence of a likely multi-dimensional response in mechanisms intrinsic to the striatum, but also possibly within other elements of the re-entrant looped architecture that connects the basal ganglia with the cerebral cortex. The current highly constrained model now offers the opportunity to investigate independently how the different elements that contribute to the overall multiunit response are modulated by precisely timed sensory reinforcement [78].

Finally, our study confirms that plasticity induced in the striatum by delayed sensory reinforcement is partly dependent on intact DA transmission. Thus, some of the observed plasticity was blocked by systemic injection of a dopaminergic D1/D5-receptor antagonist [21, 22, 34, 79-81]. Some of the potentiation was also blocked by the systemic injection of a dopaminergic D2/D3-receptor antagonist. This latter effect could in part be attributed to the blockade of a form of long term potentiation dependent on the activation of D2-type receptors and endocannabinoid-receptor signalling reported at the glutamatergic synapses formed on MSNs [71, 72]. However, in the condition where both D1-type and D2-type antagonists were administered there was clear evidence that corticostriatal transmission could, in some cases, still be modulated by sensory reinforcement. It is possible that the observed DA-independent plasticity might reflect spike-timing-dependent plasticity occurring at glutamatergic synapses formed on MSNs of the indirect pathway (t-LTP dependent on the activation of A2a adenosine receptors combined to the blockage of t-LTD dependent on D2R dopaminergic transmission) [9, 22, 34, 82]. To a lesser extent the potentiation of cortical synapses formed on striatal GABAergic interneurons could be involved [73, 74]. In addition, thalamic gating by the light flash could have also contributed to the observed plasticity. The activated thalamic input may itself modulate the activity of fast-spiking interneurons [83] or cholinergic interneurons [41], with flow-on effects to corticostriatal inputs. In future studies, optogenetic methodologies will allow temporal control over the independent activation or silencing of the afferent pathways carrying sensory information to the striatum from substantia nigra and/or the thalamus [59, 84-86]. Such studies will determine the relative importance of dopaminergic and glutamatergic transmission in the process of sensory reinforced plasticity within the striatal micro-circuit.

5. Conclusion

The current *in vivo* model of sensory-reinforcement offers a novel paradigm with which to address the

physiological, cellular and molecular bases of diverse forms of corticostriatal plasticity. An important feature of the paradigm is that it parallels significant aspects of instrumental conditioning in behaving animals [1, 17]. While caution must be exercised over the extent to which our results may have been influenced by the animals being anaesthetised, what we have been able to show is that when precisely controlled motor and sensory inputs converge on striatal units in a temporally relevant manner the response to the motor input was potentiated. The extent to which this finding generalises to awake behaving preparations is a question for the future. That said, the fact that in our *in vivo* model, behaviourally relevant afferent projections [40, 42, 45-47, 59] can be appropriately activated by a natural sensory stimulus in a reduced anaesthetized preparation [43, 44] offers a degree of experimental control that would be more difficult to achieve in awake behaving animals. While the current study was always intended as a principal demonstration of sensory reinforced striatal plasticity, having shown that it can occur with precise experimental control, there are numerous additional features of this novel paradigm that could be investigated. For example, will the current sensory-reinforced plasticity operate in the associative and limbic territories of the striatum? What are the cellular and molecular processes that occur in different striatal cell types to support the observed plasticity? Can sensory reinforcement potentiate striatal activity generated in functional territories coding for sensory information [40]? Such territories could participate in the reinforcement of contextual information in which an action leading to an unexpected outcome occurs [10]. A different line of future research would test whether variables that influence plasticity in the current model have comparable effects on behavioural reinforcement learning, conversely, whether variables known to influence the acquisition of novel actions have similar effects in the present model of plasticity. A better appreciation of the neural processes underlying reinforcement can only assist our interpretation of instances when it fails or becomes pathologically modified, as in aspects of Parkinson's disease [87], schizophrenia [88], dystonia [89] and the addictions [90]. Such understanding may also be a pre-requisite for the discovery of rational therapies for these debilitating conditions.

List of abbreviations:

DA	dopamine
GLU	glutamate
MSN	medium spiny neuron
RANOVA	random effects ANOVA
STDP	spike-timing-dependent plasticity

Author contributions: N.V. and V.C. jointly performed and analyzed the multi-unit electrophysiological experiments and immunohistochemistry, and co-drafted the manuscript. N.V. performed the antagonist studies. M.L. performed the majority of histological experiments. Y.F.Z., V.C., and J. N. J. R. performed single unit recording experiments and J.M.S. and L.D. undertook additional supporting *in vivo* electrophysiological experiments. A.Z. assisted with data analysis. P.O. and E.B. contributed to experimental design and data interpretation. J.N.J.R. and P.R. designed the experiments, drafted the manuscript, and supervised the study. All authors critically reviewed the manuscript and gave consent for publication.

Conflict of Interest: The authors declare no conflicting interests.

Acknowledgements: This work was supported by grants from the Wellcome Trust (080943 and 091409) and the Marsden Fund of the Royal Society of New Zealand (UOO0513, UOO0904, and UOO1802). Véronique Coizet and Nicolas Vautrelle contributed equally to this work. We would also like to thank Manfred Oswald and Natalie Kennerley for technical assistance, and the following for their constructive comments on an early draft of the manuscript – Jim Surmeier, Jeffrey Wickens, Atsushi Nambu, Joshua Berke, Yael Niv and Nathaniel Daw.

References

1. Thorndike EL. Animal intelligence. New York: Macmillan; 1911.
2. Bar-Gad I, Havazelet-Heimer G, Goldberg JA, Ruppin E, Bergman H. Reinforcement-driven dimensionality reduction--a model for information processing in the basal ganglia. J Basic Clin Physiol Pharmacol. 2000;11(4):305-20.
3. Cataldi S, Stanley AT, Miniaci MC, Sulzer D. Interpreting the role of the striatum during multiple phases of motor learning. FEBS J. 2021.
4. Hart G, Leung BK, Balleine BW. Dorsal and ventral streams: the distinct role of striatal subregions in the acquisition and performance of goal-directed actions. Neurobiol Learn Mem. 2014;108:104-18.
5. Redgrave P, Gurney K. The short-latency dopamine signal: a role in discovering novel actions ? Nat Rev Neurosci. 2006;7(12):967-75.
6. Redgrave P, Vautrelle N, Reynolds JN. Functional properties of the basal ganglia's re-entrant loop architecture: selection and reinforcement. Neuroscience. 2011;198:138-51.

7. Balleine BW, Delgado MR, Hikosaka O. The role of the dorsal striatum in reward and decision-making. J Neurosci. 2007;27(31):8161-5.
8. Graybiel AM. The basal ganglia: learning new tricks and loving it. Curr Opin Neurobiol. 2005;15(6):638-44.
9. Gurney KN, Humphries MD, Redgrave P. A new framework for cortico-striatal plasticity: behavioural theory meets in vitro data at the reinforcement-action interface. PLoS Biol. 2015;13(1):e1002034.
10. Redgrave P, Gurney K, Reynolds J. What is reinforced by phasic dopamine signals? Brain Res Rev. 2008;58(2):322-39.
11. Barto A, Mirolli M, Baldassarre G. Novelty or surprise? Front Psychol. 2013;4:907.
12. Bromberg-Martin ES, Matsumoto M, Hikosaka O. Dopamine in motivational control: rewarding, aversive, and alerting. Neuron. 2010;68(5):815-34.
13. Lloyd DR, Gancarz AM, Ashrafioun L, Kausch MA, Richards JB. Habituation and the reinforcing effectiveness of visual stimuli. Behav Processes. 2012;91(2):184-91.
14. Menegas W, Babayan BM, Uchida N, Watabe-Uchida M. Opposite initialization to novel cues in dopamine signaling in ventral and posterior striatum in mice. Elife. 2017;6.
15. Reynolds JNJ, Hyland BI, Wickens JR. A cellular mechanism of reward-related learning. Nature. 2001;413:67-70.
16. Schultz W. Behavioral theories and the neurophysiology of reward. Annu Rev Psychol. 2006;57:87-115.
17. Wickens JR. Synaptic plasticity in the basal ganglia. Behav Brain Res. 2009;199(1):119-28.
18. Calabresi P, Picconi B, Tozzi A, Di Filippo M. Dopamine-mediated regulation of corticostriatal synaptic plasticity. Trends Neurosci. 2007;30(5):211-9.
19. Fino E, Glowinski J, Venance L. Bidirectional activity-dependent plasticity at corticostriatal synapses. J Neurosci. 2005;25(49):11279-87.
20. Fino E, Venance L. Spike-timing dependent plasticity in the striatum. Front Synaptic Neurosci. 2010;2:6.
21. Pawlak V, Kerr JN. Dopamine receptor activation is required for corticostriatal spike-timing-dependent plasticity. J Neurosci. 2008;28(10):2435-46.
22. Shen WX, Flajolet M, Greengard P, Surmeier DJ. Dichotomous dopaminergic control of striatal synaptic plasticity. Science. 2008;321(5890):848-51.
23. Dickinson A. The 28th Bartlett Memorial Lecture Causal learning: An associative analysis. Quart J Exp Psych B Com Phy P. 2001;54:3-25.

24. Foncelle A, Mendes A, Jedrzejewska-Szmek J, Valtcheva S, Berry H, Blackwell KT, et al. Modulation of spike-timing dependent plasticity: towards the inclusion of a third factor in computational models. Front Comput Neurosci. 2018;12:49.

25. Fremaux N, Gerstner W. Neuromodulated spike-timing-dependent plasticity, and theory of three-factor learning rules. Front Neural Circuits. 2015;9:85.

26. Izhikevich EM. Solving the distal reward problem through linkage of STDP and dopamine signaling. Cereb Cortex. 2007;17(10):2443-52.

27. Cacciapaglia F, Saddoris MP, Wightman RM, Carelli RM. Differential dopamine release dynamics in the nucleus accumbens core and shell track distinct aspects of goal-directed behavior for sucrose. Neuropharmacology. 2012;62(5-6):2050-6.

28. Howard CD, Li H, Geddes CE, Jin X. Dynamic nigrostriatal dopamine biases action selection. Neuron. 2017;93(6):1436-50 e8.

29. Phillips PE, Stuber GD, Heien ML, Wightman RM, Carelli RM. Subsecond dopamine release promotes cocaine seeking. Nature. 2003;422(6932):614-8.

30. Roitman MF, Stuber GD, Phillips PE, Wightman RM, Carelli RM. Dopamine operates as a subsecond modulator of food seeking. J Neurosci. 2004;24(6):1265-71.

31. Stopper CM, Tse MTL, Montes DR, Wiedman CR, Floresco SB. Overriding phasic dopamine signals redirects action selection during risk/reward decision making. Neuron. 2014;84(1):177-89.

32. Stuber GD, Roitman MF, Phillips PE, Carelli RM, Wightman RM. Rapid dopamine signaling in the nucleus accumbens during contingent and noncontingent cocaine administration. Neuropsychopharmacology. 2005;30(5):853-63.

33. Yagishita S, Hayashi-Takagi A, Ellis-Davies GC, Urakubo H, Ishii S, Kasai H. A critical time window for dopamine actions on the structural plasticity of dendritic spines. Science. 2014;345(6204):1616-20.

34. Fisher SD, Robertson PB, Black MJ, Redgrave P, Sagar MA, Abraham WC, et al. Reinforcement determines the timing dependence of corticostriatal synaptic plasticity in vivo. Nat Commun. 2017;8(1):334.

35. Schulz JM, Redgrave P, Reynolds JN. Cortico-striatal spike-timing dependent plasticity after activation of subcortical pathways. Front Synaptic Neurosci. 2010;2:23.

36. Shindou T, Shindou M, Watanabe S, Wickens J. A silent eligibility trace enables dopamine-dependent synaptic plasticity for reinforcement learning in the mouse striatum. Eur J Neurosci. 2019;49(5):726-36.

37. Reynolds JNJ, Avvisati R, Dodson PD, Fisher SD, Oswald MJ, Wickens JR, et al. Coincidence of cholinergic pauses, dopaminergic activation and depolarisation of spiny projection neurons drives synaptic plasticity in the striatum. Nat Comms. 2022;13(1):1296.

38. Gerstner W, Lehmann M, Liakoni V, Corneil D, Brea J. Eligibility traces and plasticity on behavioral time scales: experimental support of neoHebbian three-Factor learning rules. Front Neural Circuits. 2018;12:53.

39. Reiner A, Jiao Y, DelMar N, Laverghetta AV, Lei WL. Differential morphology of pyramidal tract-type and intratelencephalically projecting-type corticostriatal neurons and their intrastriatal terminals in rats. J Comp Neurol. 2003;457:420-40.

40. Hunnicutt BJ, Jongbloets BC, Birdsong WT, Gertz KJ, Zhong H, Mao T. A comprehensive excitatory input map of the striatum reveals novel functional organization. Elife. 2016;5.

41. Ding JB, Guzman JN, Peterson JD, Goldberg JA, Surmeier DJ. Thalamic Gating of Corticostriatal Signaling by Cholinergic Interneurons. Neuron. 2010;67(2):294-307.

42. Matsumoto N, Minamimoto T, Graybiel AM, Kimura M. Neurons in the thalamic CM-Pf complex supply striatal neurons with information about behaviorally significant sensory events. Journal of Neurophysiology. 2001;85:960-76.

43. Schulz JM, Redgrave P, Mehring C, Aertsen A, Clements KM, Wickens JR, et al. Short-latency activation of striatal spiny neurons via subcortical visual pathways. J Neurosci. 2009;29(19):6336-47.

44. Dommett E, Coizet V, Blaha CD, Martindale J, Lefebvre V, Walton N, et al. How visual stimuli activate dopaminergic neurons at short latency. Science. 2005;307(5714):1476-9.

45. Benavidez NL, Bienkowski MS, Zhu M, Garcia LH, Fayzullina M, Gao L, et al. Organization of the inputs and outputs of the mouse superior colliculus. Nat Commun. 2021;12(1):4004.

46. Coizet V, Overton PG, Redgrave P. Collateralization of the tectonigral projection with other major output pathways of superior colliculus in the rat. J Comp Neurol. 2007;500(6):1034-49.

47. Comoli E, Coizet V, Boyes J, Bolam JP, Canteras NS, Quirk RH, et al. A direct projection from superior colliculus to substantia nigra for detecting salient visual events. Nat Neurosci. 2003;6(9):974-80.

48. Valjent E, Pascoli V, Svenningsson P, Paul S, Enslen H, Corvol JC, et al. Regulation of a protein phosphatase cascade allows convergent dopamine and glutamate signals to activate ERK in the striatum. Proc Natl Acad Sci U S A. 2005;102(2):491-6.

49. Katsuta H, Isa T. Release from GABA(A) receptor-mediated inhibition unmasks interlaminar connection within superior colliculus in anesthetized adult rats. Neurosci Res. 2003;46(1):73-83.

50. Sgambato V, Abo V, Rogard M, Besson MJ, Deniau JM. Effect of electrical stimulation of the cerebral cortex on the expression of the Fos protein in the basal ganglia. Neuroscience. 1997;81:93-112.

51. Manly BFJ. Randomization and Monte Carlo methods in biology. 1st edition ed. London: Chapman and Hall; 1991. 281 p.

52. Coizet V, Graham JH, Moss J, Bolam JP, Savasta M, McHaffie JG, et al. Short-latency visual input to the subthalamic nucleus is provided by the midbrain superior colliculus. J Neurosci. 2009;29(17):5701-9.

53. Alexander GE, DeLong MR, Strick PL. Parallel organization of functionally segregated circuits linking basal ganglia and cortex. Ann Rev Neurosci. 1986;9:357-81.

54. McHaffie JG, Stanford TR, Stein BE, Coizet V, Redgrave P. Subcortical loops through the basal ganglia. Trends Neurosci. 2005;28(8):401-7.

55. Wilson CJ. Postsynaptic potentials evoked in spiny neostriatal projection neurons by stimulation of ipsilateral and contralateral neocortex. Brain Res. 1986;367(1-2):201-13.

56. Brown JR, Arbuthnott GW. The electrophysiology of dopamine (D2) receptors: a study of the actions of dopamine on corticostriatal transmission. Neuroscience. 1983;10(2):349-55.

57. Balleine BW, Lijeholm M, Ostlund SB. The integrative function of the basal ganglia in instrumental conditioning. Behav Brain Res. 2009;199(1):43-52.

58. Peak J, Hart G, Balleine BW. From learning to action: the integration of dorsal striatal input and output pathways in instrumental conditioning. Eur J Neurosci. 2019;49(5):658-71.

59. Kato S, Fukabori R, Nishizawa K, Okada K, Yoshioka N, Sugawara M, et al. Action selection and flexible switching controlled by the intralaminar thalamic neurons. Cell Rep. 2018;22(9):2370-82.

60. Klaus A, Alves da Silva J, Costa RM. What, if, and when to move: Basal ganglia circuits and self-paced action initiation. Annu Rev Neurosci. 2019;42:459-83.

61. Mink JW. The basal ganglia: Focused selection and inhibition of competing motor programs. Prog Neurobiol. 1996;50:381-425.

62. Redgrave P, Prescott T, Gurney KN. The basal ganglia: A vertebrate solution to the selection problem ? Neuroscience. 1999;89:1009-23.

63. Chevalier G, Deniau JM. Disinhibition as a basic process in the expression of striatal functions. Trends Neurosci. 1990;13:277-81.

64. Humphries MD, Stewart RD, Gurney KN. A physiologically plausible model of action selection and oscillatory activity in the basal ganglia. J Neurosci. 2006;26(50):12921-42.

65. Prescott TJ, Gonzalez FMM, Gurney K, Humphries MD, Redgrave P. A robot model of the basal ganglia: Behavior and intrinsic processing. Neural Netw. 2006;19(1):31-61.

66. Arbuthnott GW, Wickens J. Space, time and dopamine. Trends Neurosci. 2007;30(2):62-9.

67. Menegas W, Bergan JF, Ogawa SK, Isogai Y, Umadevi Venkataraju K, Osten P, et al. Dopamine neurons projecting to the posterior striatum form an anatomically distinct subclass. Elife. 2015;4:e10032.

68. Schultz W. Predictive reward signal of dopamine neurons. J Neurophysiol. 1998;80:1-27.

69. Van der Werf YD, Witter MP, Groenewegen HJ. The intralaminar and midline nuclei of the thalamus. Anatomical and functional evidence for participation in processes of arousal and awareness. Brain Res Rev. 2002;39:107-40.

70. Fino E, Deniau JM, Venance L. Brief subthreshold events can act as Hebbian signals for long-term plasticity. PLoS One. 2009;4(7).

71. Cui Y, Paille V, Xu H, Genet S, Delord B, Fino E, et al. Endocannabinoids mediate bidirectional striatal spike-timing-dependent plasticity. J Physiol. 2015;593(13):2833-49.

72. Cui Y, Prokin I, Xu H, Delord B, Genet S, Venance L, et al. Endocannabinoid dynamics gate spike-timing dependent depression and potentiation. Elife. 2016;5:e13185.

73. Fino E, Deniau JM, Venance L. Cell-specific spike-timing-dependent plasticity in GABAergic and cholinergic interneurons in corticostriatal rat brain slices. J Physiol. 2008;586(1):265-82.

74. Fino E, Paille V, Deniau JM, Venance L. Asymmetric spike-timing dependent plasticity of striatal nitric oxide-synthase interneurons. Neuroscience. 2009;160(4):744-54.

75. Peters AJ, Fabre JMJ, Steinmetz NA, Harris KD, Carandini M. Striatal activity topographically reflects cortical activity. Nature. 2021;591(7850):420-5.

76. Sharott A, Doig NM, Mallet N, Magill PJ. Relationships between the firing of identified striatal interneurons and spontaneous and driven cortical activities in vivo. J Neurosci. 2012;32(38):13221-36.

77. Sharott A, Moll CK, Engler G, Denker M, Grun S, Engel AK. Different subtypes of striatal neurons are selectively modulated by cortical oscillations. J Neurosci. 2009;29(14):4571-85.

78. Martiros N, Burgess AA, Graybiel AM. Inversely active striatal projection neurons and interneurons selectively delimit useful behavioral sequences. Curr Biol. 2018;28(4):560-73 e5.

79. Centonze D, Grande C, Saulle E, Martin AB, Gubellini P, Pavon N, et al. Distinct roles of D1 and D5 dopamine receptors in motor activity and striatal synaptic plasticity. J Neurosci. 2003;23(24):8506-12.

80. Kerr JN, Wickens JR. Dopamine D-1/D-5 receptor activation is required for long-term potentiation in the rat neostriatum in vitro. Journal of Neurophysiology. 2001;85(1):117-24.

81. Suzuki T, Miura M, Nishimura K, Aosaki T. Dopamine-dependent synaptic plasticity in the striatal cholinergic interneurons. J Neurosci. 2001;21(17):6492-501.

82. Flajolet M, Wang Z, Futter M, Shen W, Nuangchamnong N, Bendor J, et al. FGF acts as a co-transmitter through adenosine A(2A) receptor to regulate synaptic plasticity. Nat Neurosci. 2008;11(12):1402-9.

83. Sciamanna G, Ponterio G, Mandolesi G, Bonsi P, Pisani A. Optogenetic stimulation reveals distinct modulatory properties of thalamostriatal vs corticostriatal glutamatergic inputs to fast-spiking interneurons. Sci Rep. 2015;5:16742.

84. Saunders BT, Richard JM, Margolis EB, Janak PH. Dopamine neurons create Pavlovian conditioned stimuli with circuit-defined motivational properties. Nat Neurosci. 2018;21(8):1072-83.

85. Saunders BT, Richard JM, Janak PH. Contemporary approaches to neural circuit manipulation and mapping: focus on reward and addiction. Philos Trans R Soc Lond B Biol Sci. 2015;370(1677):20140210.

86. Huang M, Li D, Cheng X, Pei Q, Xie Z, Gu H, et al. The tectonigral pathway regulates appetitive locomotion in predatory hunting in mice. Nat Commun. 2021;12(1):4409.

87. Voon V, Fernagut PO, Wickens J, Baunez C, Rodriguez M, Pavon N, et al. Chronic dopaminergic stimulation in Parkinson's disease: from dyskinesias to impulse control disorders. Lancet Neurology. 2009;8(12):1140-9.

88. Ziauddeen H, Murray GK. The relevance of reward pathways for schizophrenia. Curr Opin Psychiatr. 2010;23(2):91-6.

89. Sciamanna G, Tassone A, Mandolesi G, Puglisi F, Ponterio G, Martella G, et al. Cholinergic dysfunction alters synaptic integration between thalamostriatal and corticostriatal inputs in DYT1 dystonia. J Neurosci. 2012;32(35):11991-2004.

90. Russo SJ, Dietz DM, Dumitriu D, Morrison JH, Malenka RC, Nestler EJ. The addicted synapse: mechanisms of synaptic and structural plasticity in nucleus accumbens. Trends Neurosci. 2010;33(6):267-76.

Figures

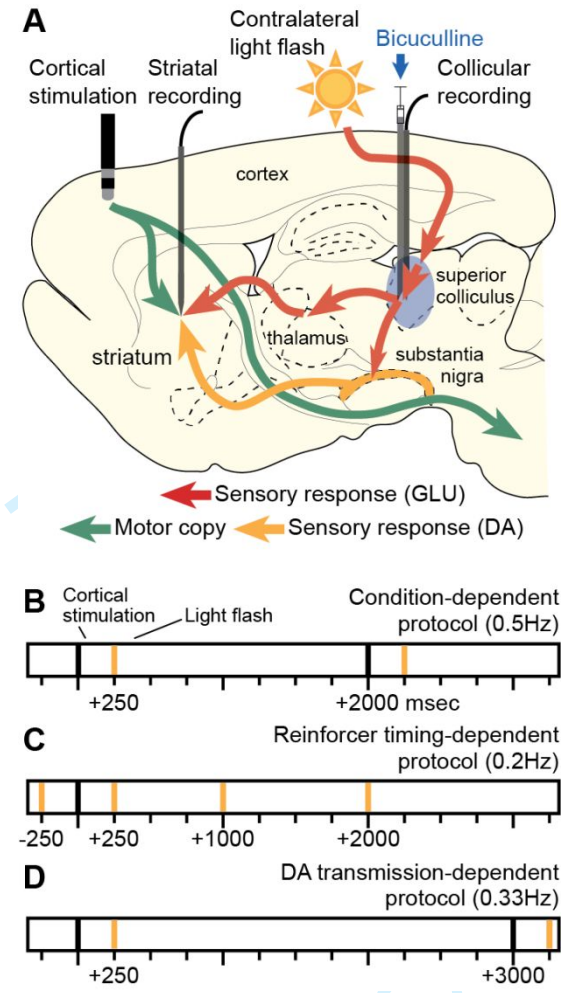

Fig. 1: Experimental paradigm and protocols. **(A)** An experimental paradigm to demonstrate sensory-reinforced corticostriatal plasticity. (i) Single electrical pulses were delivered to ipsilateral motor cortex (0.1 ms; 0.2-1.0 mA; 0.2-0.5 Hz). Sensory reinforcement relayed via the thalamostriatal (ii) and nigrostriatal (iii) projections was provided by a contralateral light flash delayed by 250 ms in the presence of a disinhibitory injection of the $GABA_A$ antagonist (bicuculline, 50ng/ 500nl) into the superior colliculus. **(B, C & D)** The timing of stimuli in the three experimental protocols. **B.** In the first set of experiments, motor cortex stimulation (black bars) was delivered with an average frequency of 0.5 Hz (ISI 30% jittered – range 1.4 to 2.6 sec). A reinforcing whole-field light flash (yellow bars) delayed by + 250 ms was paired with each cortical stimulation. **C.** In the second set of experiments, cortical stimulation (black bar) was applied at 0.2 Hz on average (ISI 30% jittered). The timing of the reinforcing light flash (yellow bars) was systematically varied to occur either before (-250 ms) or after (+250, +1000, +2000 ms) each cortical stimulation. **D.** In a third set of experiments, cortical stimulation (black bars) was delivered at an

average frequency of 0.33 Hz (ISI 30% jittered). A reinforcing whole-field light flash (yellow bars) delayed by + 250 ms was paired with each cortical stimulation.

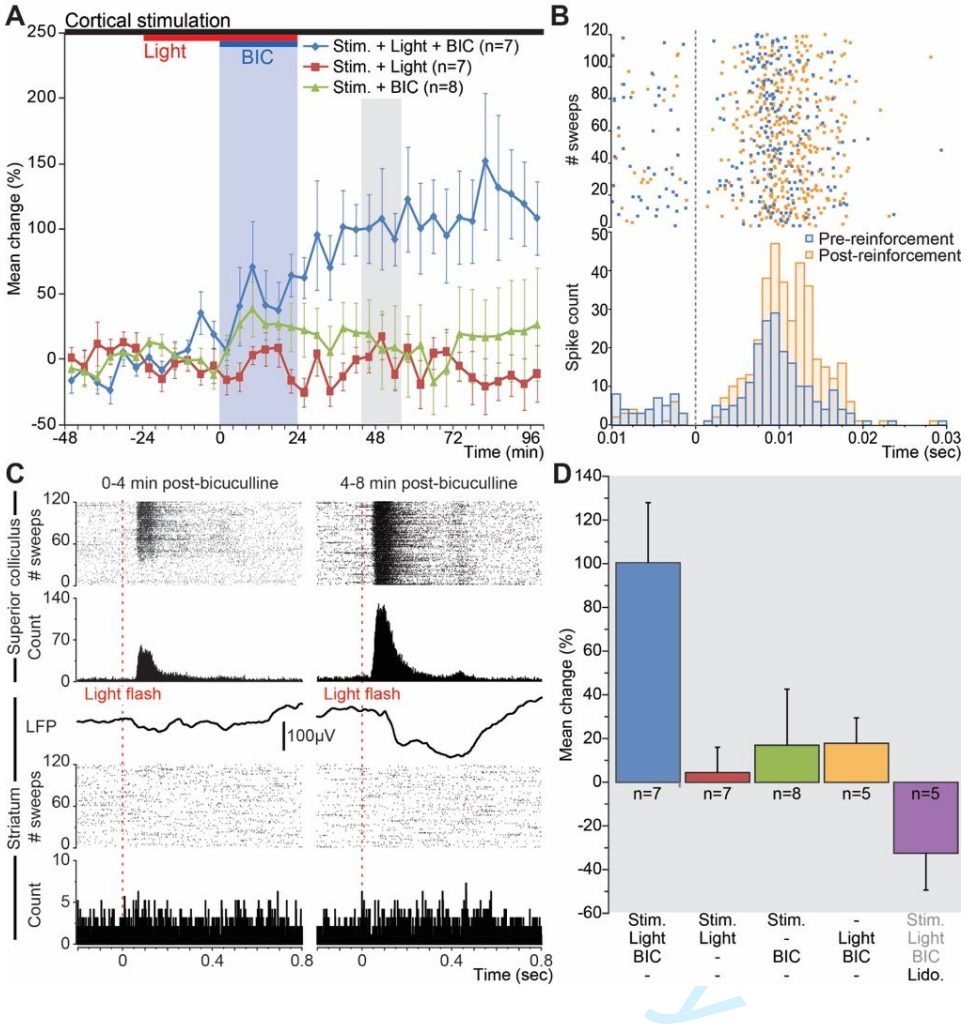

Fig. 2: Sensory-reinforced corticostriatal plasticity. **A.** Single cortical pulses (0.5 Hz) were presented throughout (black bar). Presentation of the reinforcing light flash (+250 ms) is indicated by the red bar. Dishinibition of the superior colliculus is indicated by the blue shading. Each point represents the mean change (%) in the magnitude of striatal multi-unit responses. **B.** A single case example of striatal multi-unit potentiation (raster plots and associated peri-stimulus histograms) **C.** Visual reinforcement failed to evoke spiking responses in the striatum. Bicuculline-induced restoration of visual responses to deep layer collicular neurons (top graphs); visually-evoked striatal local field potential (middle graphs); striatal multi-unit spiking (bottom graphs). **D.** For all experimental conditions, mean change (%) in the magnitude of the cortical stimulus-evoked striatal responses 44-56min after collicular disinhibition (grey shaded area in **A**). Experimental conditions are below figure.

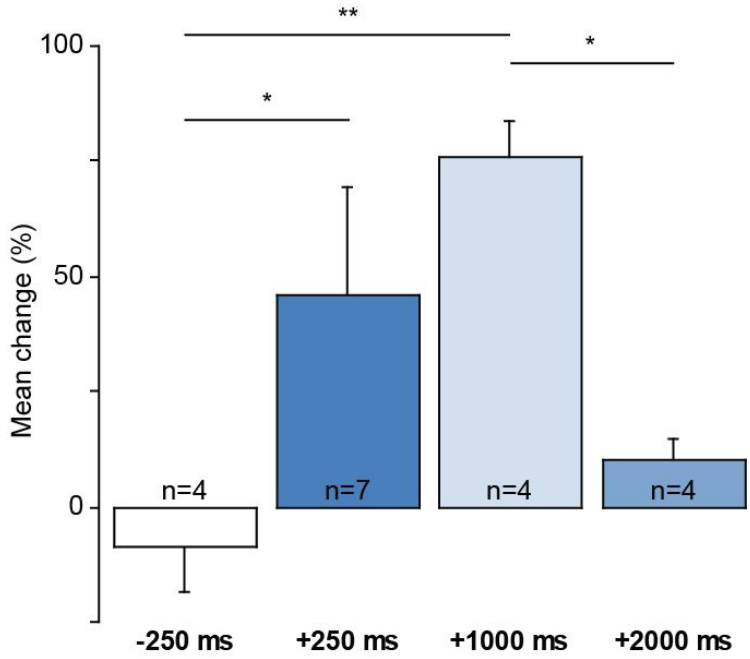

Fig. 3: Sensory reinforcement within a behaviorally relevant time window. Only when light reinforcement was delivered +250 and +1000 ms after the cortical stimulus was significant potentiation of the evoked striatal response observed (Two-way ANOVA: $F_{3,15} = 3.6$; $P < 0.04$, Fisher's PLSD test: * $P < 0.05$, ** $P < 0.01$).

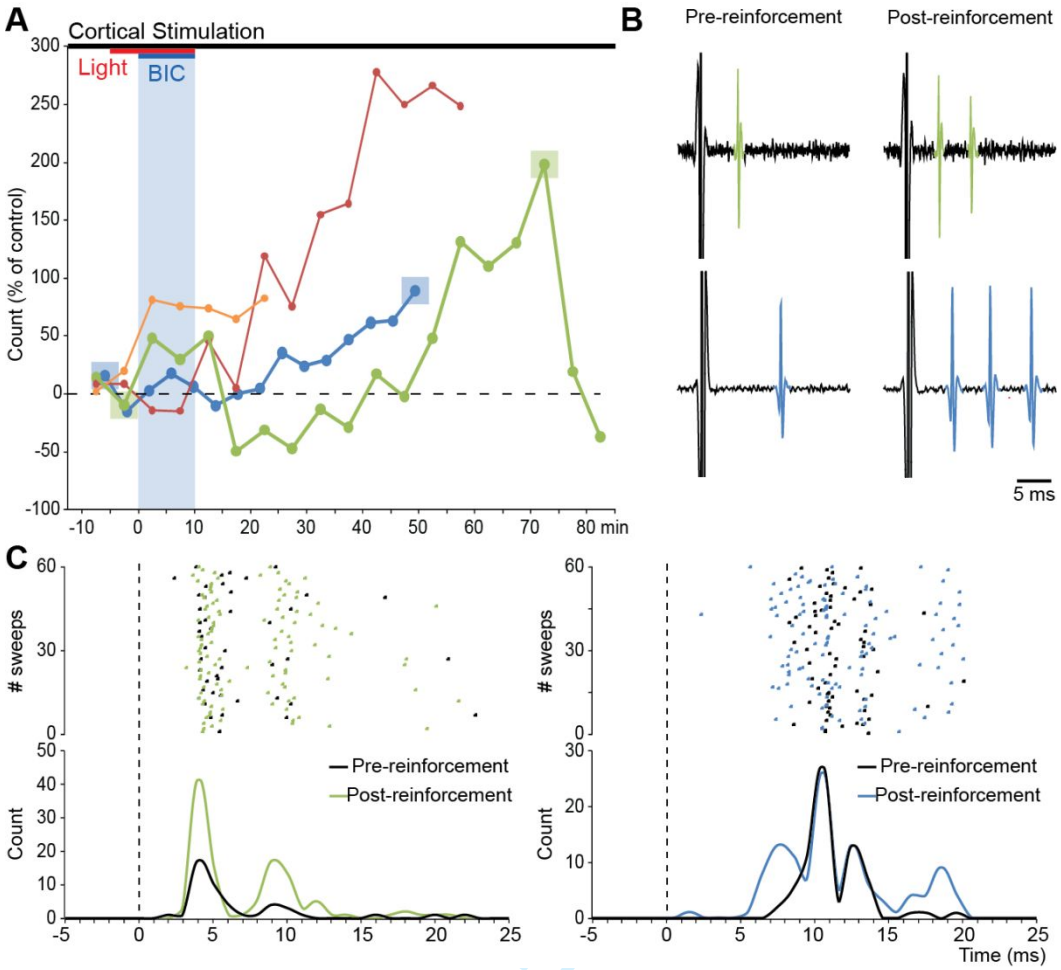

Fig. 4: Changes in neuronal activity underlying sensory-reinforced corticostriatal plasticity. **A.** Four examples of varied responses of individual neurons (different colored lines). For two neurons (dark blue and green lines), the squares mark the trials of cortical stimulation from which raster and histogram figures were calculated in **C**. **B.** Examples of pre- and post-reinforcement activity of the two single units whose data are plotted in C. **C.** In one case (green) spiking occurred more frequently at the same latencies after sensory reinforcement, while in the other case (blue) responses at some latencies remained unaltered while spiking at new shorter latencies appeared following potentiation.

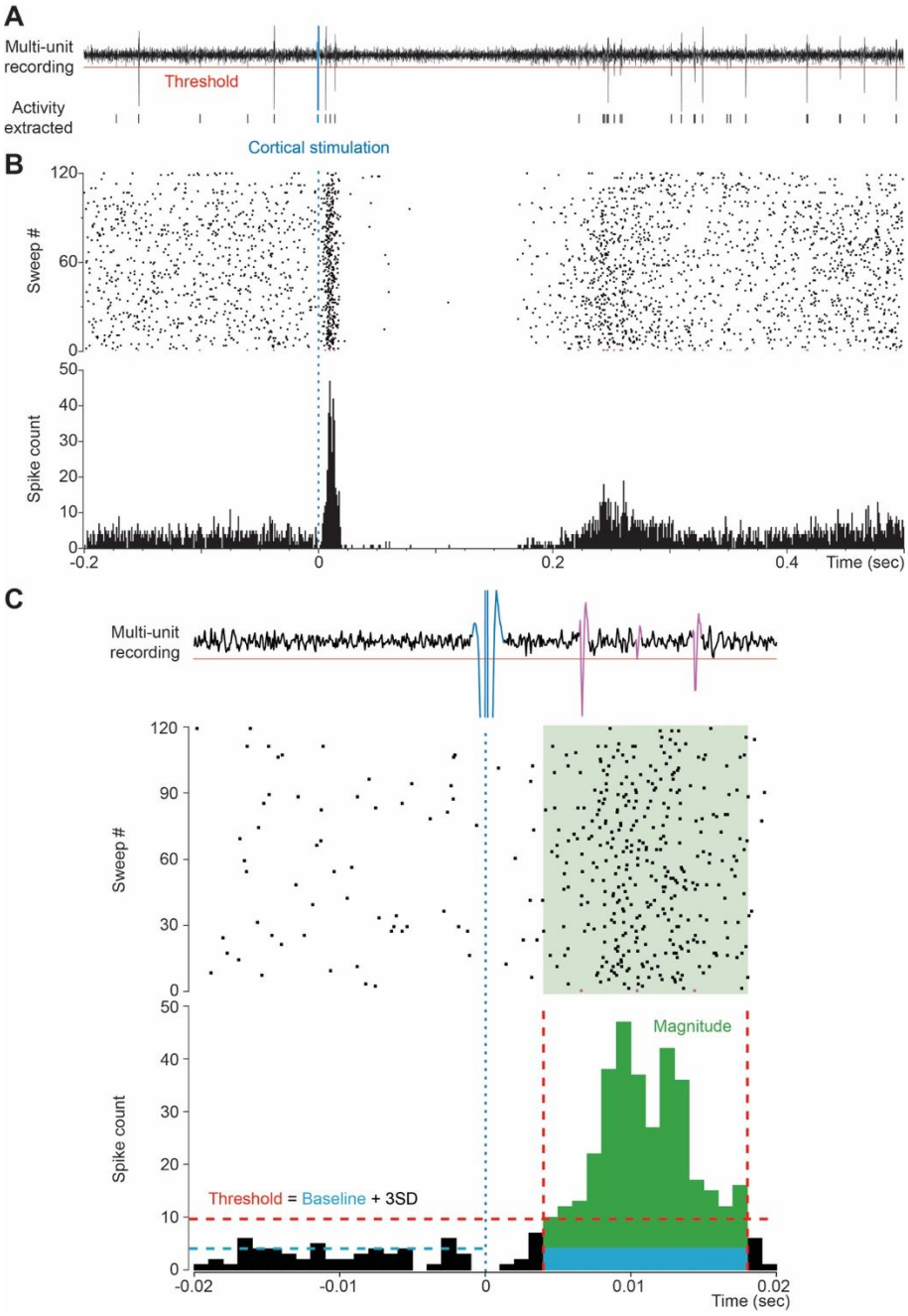

Fig. 5: Analysis of multi-unit recording. **A.** Multi-unit spike activity evoked by the cortical stimulus and the light flash were recorded locally in the striatum. **B.** Data were processed in the form of spike-count rasters and peri-stimulus histograms. **C.** Multi-unit striatal responses were recorded in successive blocks of 120 cortical stimulations. For each block multi-unit response characteristics were determined from the peri-stimulus histograms (bin width 1 ms). Response duration was determined by considering the consecutive bins when the firing rate exceeded 3SD (red dotted lines) over the mean base-line firing rate (blue dotted line). Response magnitude (green) for each block of 120 stimulations was recorded as the number of counts during the response minus the mean baseline count for the same period (blue).

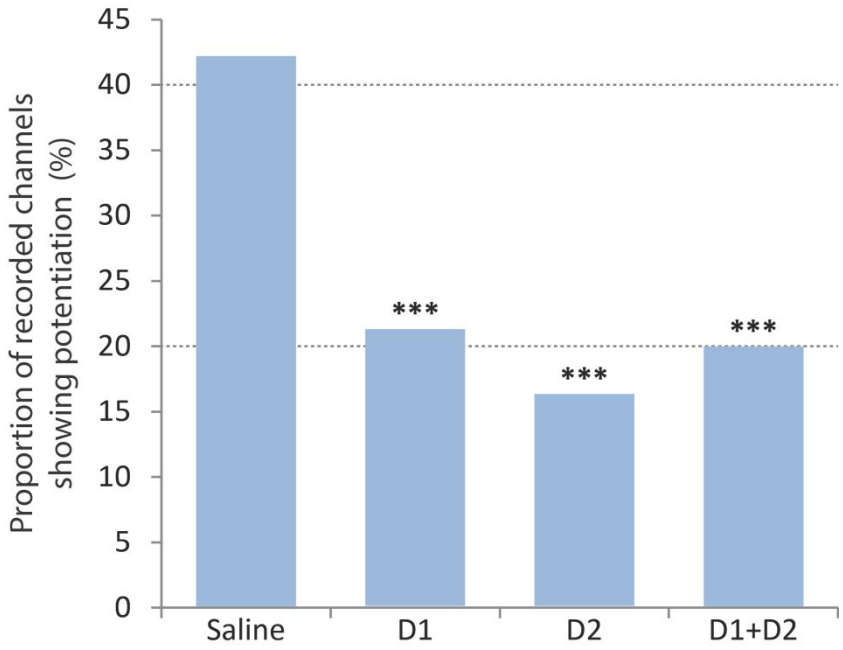

Fig. 6: Effect of blocking dopamine neurotransmission on sensory-reinforced corticostriatal plasticity. Separate and combined blockade of D1-type and D2-type dopamine receptors reduced the proportion (%) of recorded channels showing potentiation (*** Chi-square = $p<0.001$ compared with Saline group).

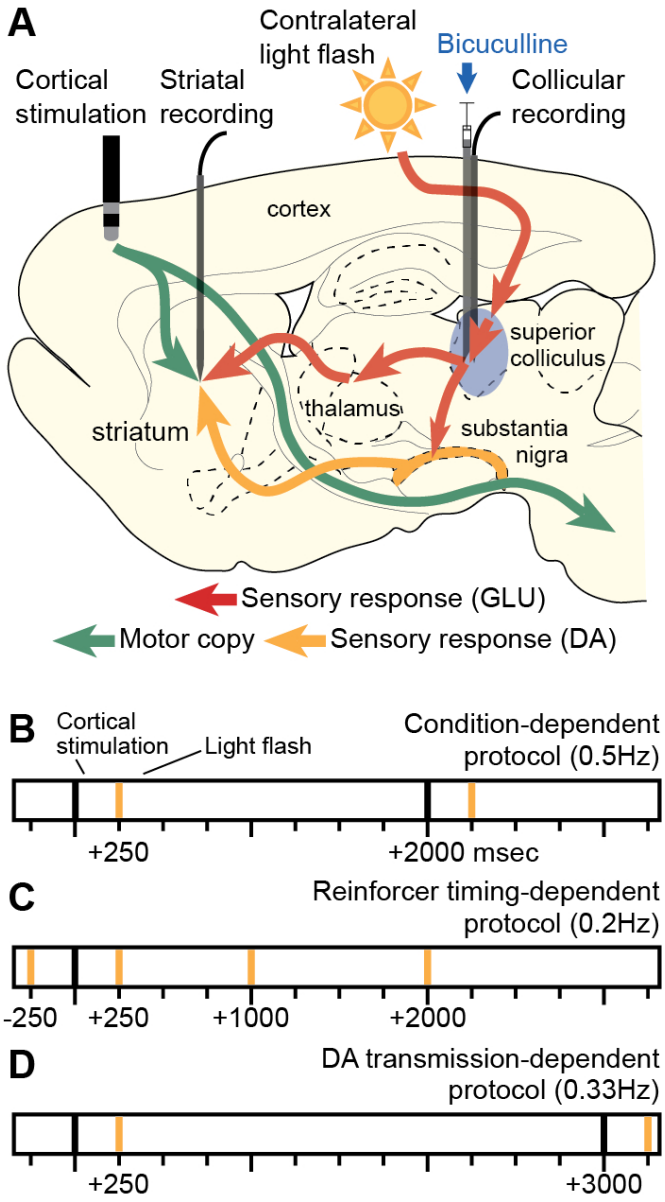

Fig. 1: Experimental paradigm and protocols. (A) An experimental paradigm to demonstrate sensory-reinforced corticostriatal plasticity. (i) Single electrical pulses were delivered to ipsilateral motor cortex (0.1 ms; 0.2-1.0 mA; 0.2-0.5 Hz). Sensory reinforcement relayed via the thalamostriatal (ii) and nigrostriatal (iii) projections was provided by a contralateral light flash delayed by 250 ms in the presence of a disinhibitory injection of the GABAA antagonist (bicuculline, 50ng/ 500nl) into the superior colliculus. (B, C & D) The timing of stimuli in the three experimental protocols. B. In the first set of experiments, motor cortex stimulation (black bars) was delivered with an average frequency of 0.5 Hz (ISI 30% jittered – range 1.4 to 2.6 sec). A reinforcing whole-field light flash (yellow bars) delayed by + 250 ms was paired with each cortical stimulation. C. In the second set of experiments, cortical stimulation (black bar) was applied at 0.2 Hz on average (ISI 30% jittered). The timing of the reinforcing light flash (yellow bars) was systematically varied to occur either before (-250 ms) or after (+250, +1000, +2000 ms) each cortical stimulation. D. In a third set of experiments, cortical stimulation (black bars) was delivered at an average frequency of 0.33 Hz (ISI 30% jittered). A reinforcing whole-field light flash (yellow bars) delayed by + 250 ms was paired with each cortical stimulation.

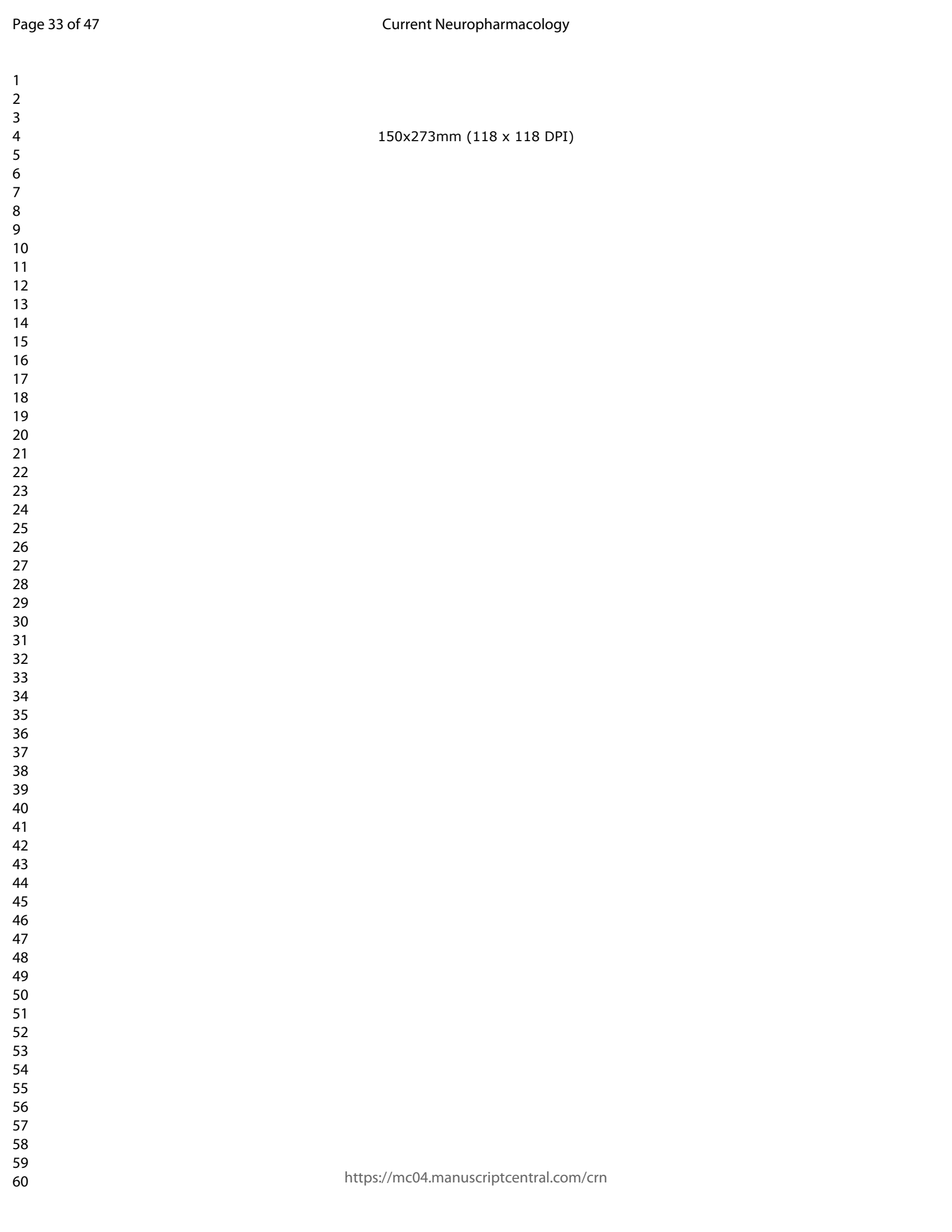
150x273mm (118 x 118 DPI)

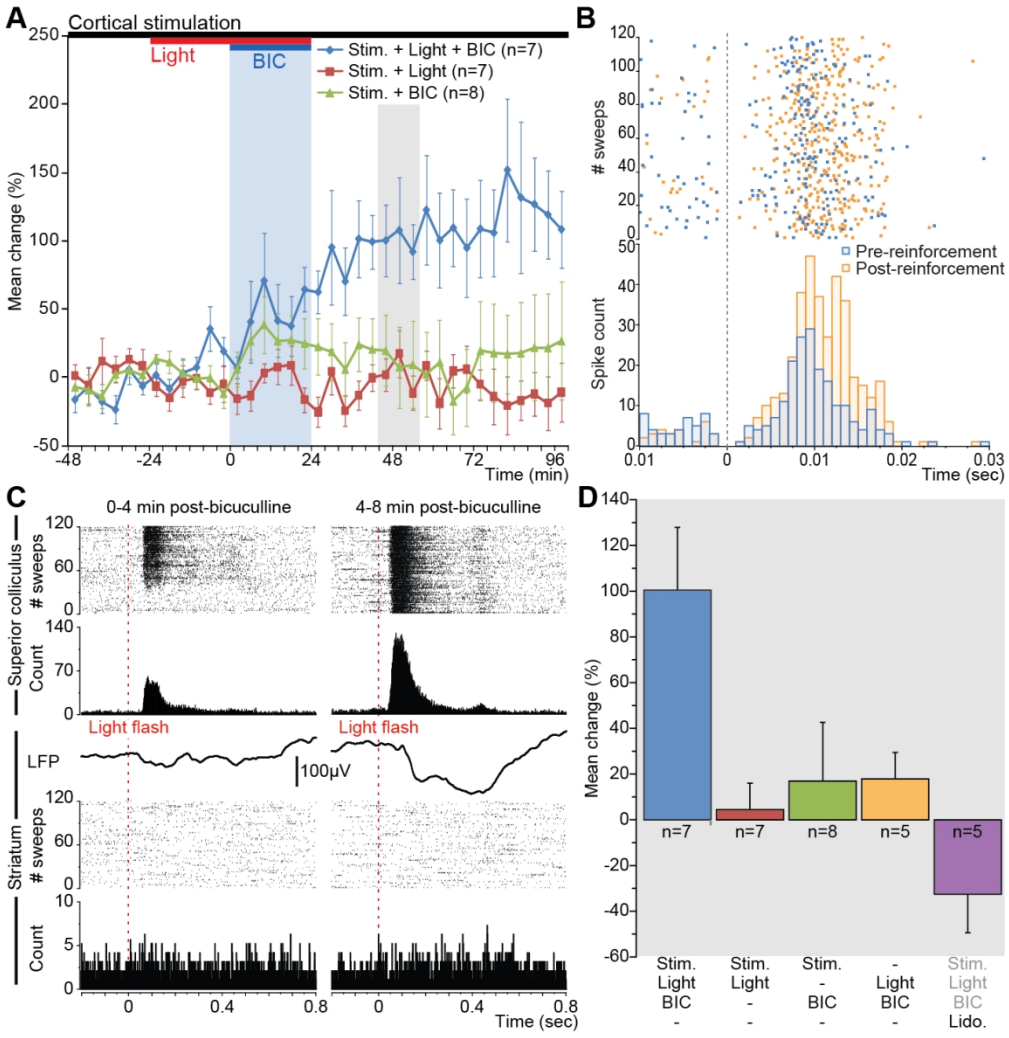

Fig. 2: Sensory-reinforced corticostriatal plasticity. A. Single cortical pulses (0.5 Hz) were presented throughout (black bar). Presentation of the reinforcing light flash (+250 ms) is indicated by the red bar. Dishinibition of the superior colliculus is indicated by the blue shading. Each point represents the mean change (%) in the magnitude of striatal multi-unit responses. B. A single case example of striatal multi-unit potentiation (raster plots and associated peri-stimulus histograms) C. Visual reinforcement failed to evoke spiking responses in the striatum. Bicuculline-induced restoration of visual responses to deep layer collicular neurons (top graphs); visually-evoked striatal local field potential (middle graphs); striatal multi-unit spiking (bottom graphs). D. For all experimental conditions, mean change (%) in the magnitude of the cortical stimulus-evoked striatal responses 44-56min after collicular disinhibition (grey shaded area in A). Experimental conditions are below figure.

305x314mm (118 x 118 DPI)

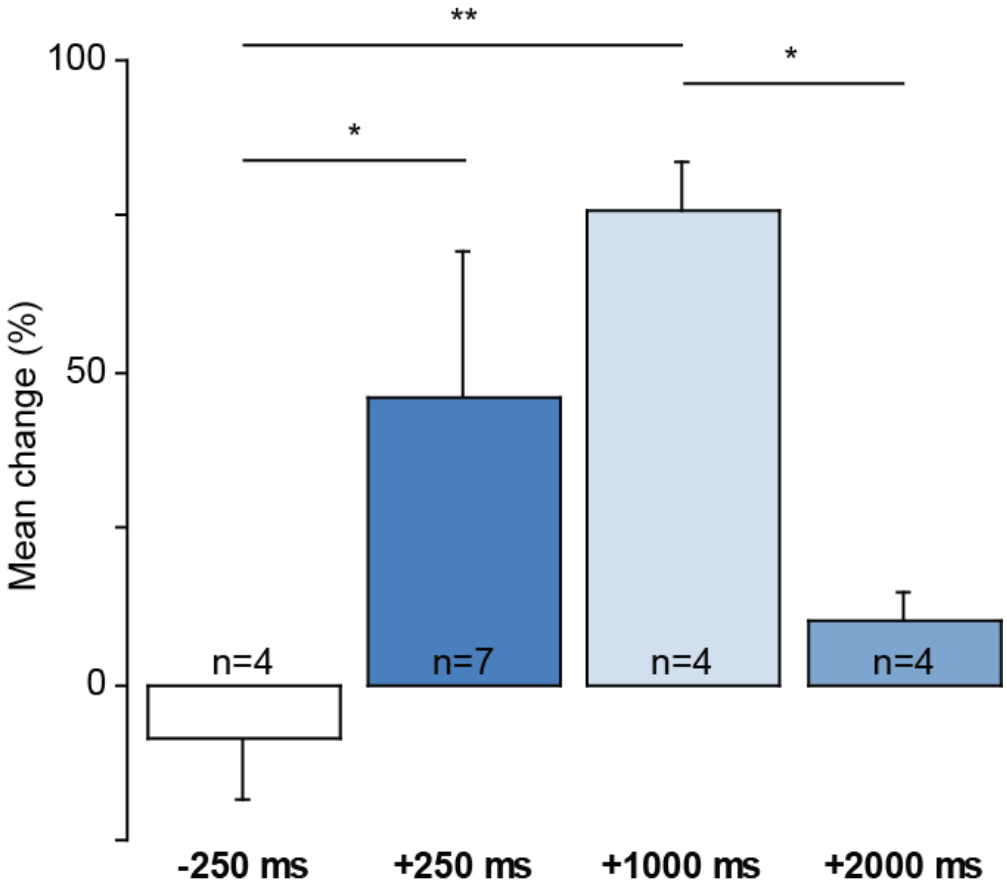

Fig. 3: Sensory reinforcement within a behaviorally relevant time window. Only when light reinforcement was delivered +250 and +1000 ms after the cortical stimulus was significant potentiation of the evoked striatal response observed (Two-way ANOVA: $F_{3,15} = 3.6$; $P < 0.04$, Fisher's PLSD test: * $P < 0.05$, ** $P < 0.01$).

145x129mm (118 x 118 DPI)

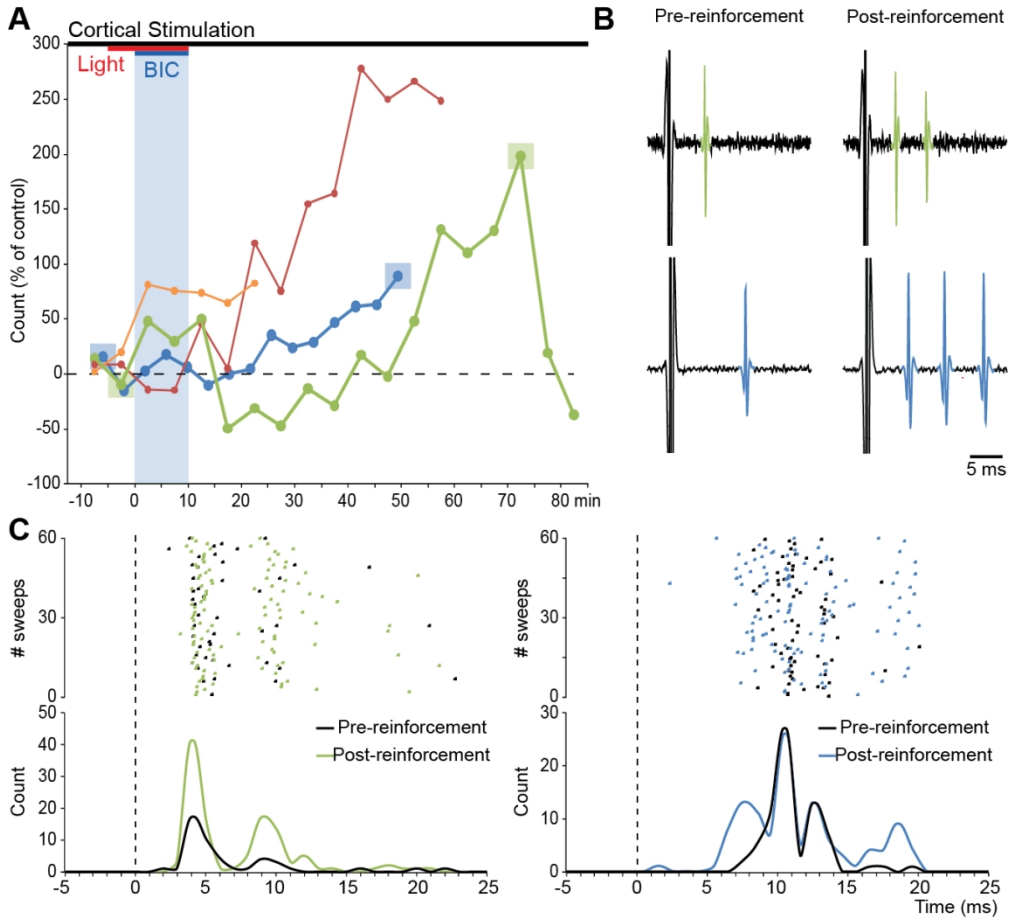

Fig. 4: Changes in neuronal activity underlying sensory-reinforced corticostriatal plasticity. A. Four examples of varied responses of individual neurons (different colored lines). For two neurons (dark blue and green lines), the squares mark the trials of cortical stimulation from which raster and histogram figures were calculated in C. B. Examples of pre- and post-reinforcement activity of the two single units whose data are plotted in C. C. In one case (green) spiking occurred more frequently at the same latencies after sensory reinforcement, while in the other case (blue) responses at some latencies remained unaltered while spiking at new shorter latencies appeared following potentiation.

288x264mm (118 x 118 DPI)

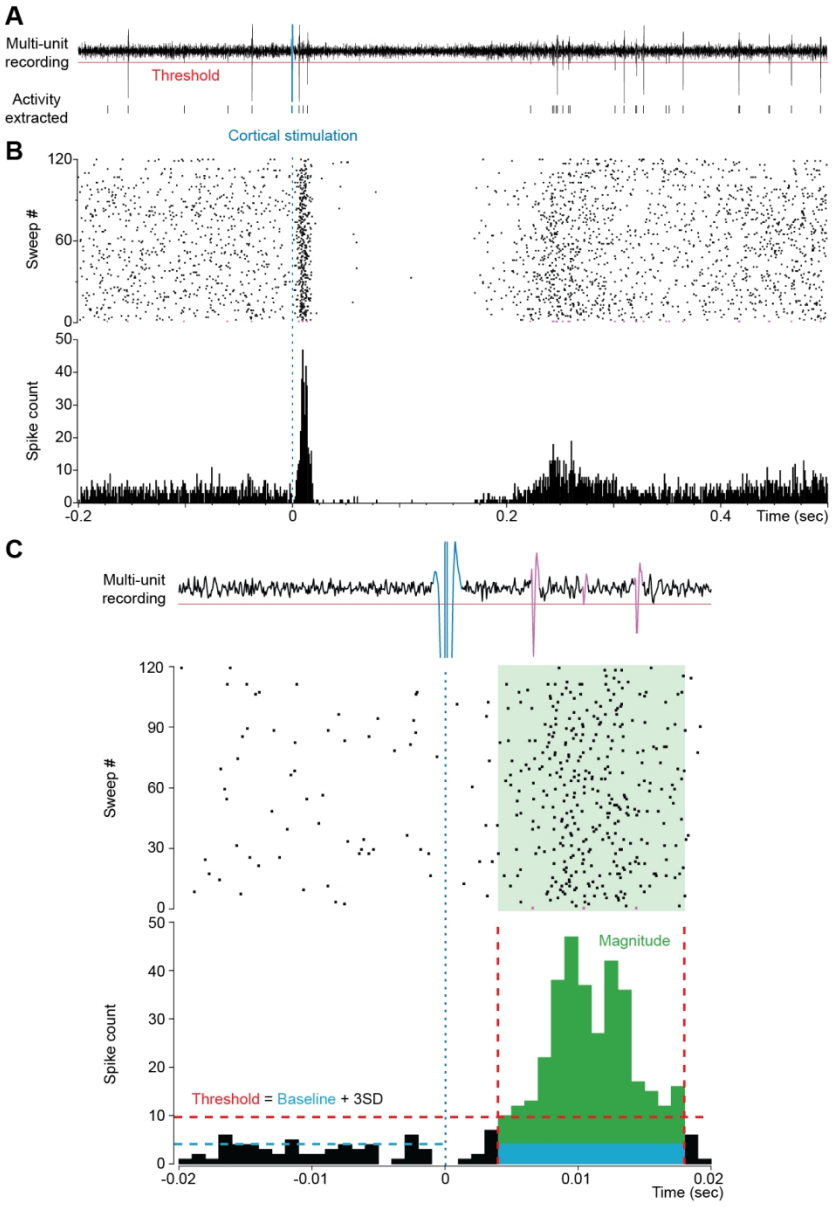

Fig. 5: Analysis of multi-unit recording. A. Multi-unit spike activity evoked by the cortical stimulus and the light flash were recorded locally in the striatum. B. Data were processed in the form of spike-count rasters and peri-stimulus histograms. C. Multi-unit striatal responses were recorded in successive blocks of 120 cortical stimulations. For each block multi-unit response characteristics were determined from the peri-stimulus histograms (bin width 1 ms). Response duration was determined by considering the consecutive bins when the firing rate exceeded 3SD (red dotted lines) over the mean base-line firing rate (blue dotted line). Response magnitude (green) for each block of 120 stimulations was recorded as the number of counts during the response minus the mean baseline count for the same period (blue).

289x421mm (118 x 118 DPI)

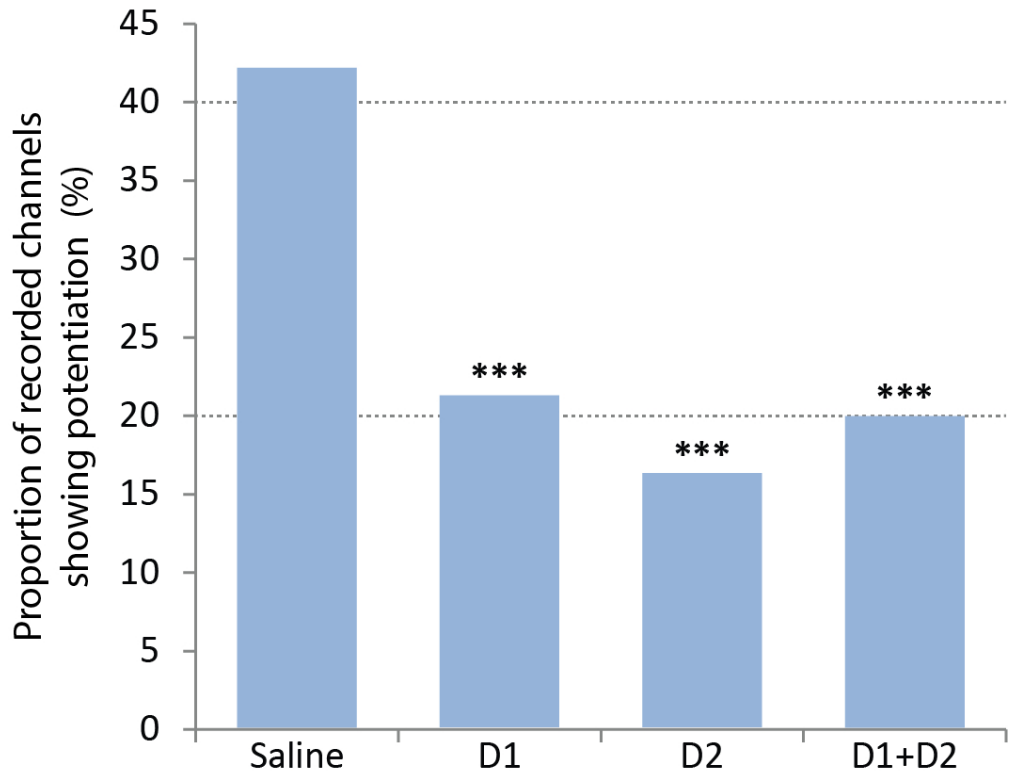

Fig. 6: Effect of blocking dopamine neurotransmission on sensory-reinforced corticostriatal plasticity. Separate and combined blockade of D1-type and D2-type dopamine receptors reduced the proportion (%) of recorded channels showing potentiation (*** Chi-square = $p<0.001$ compared with Saline group).

228x178mm (118 x 118 DPI)

Supplementary Material for:

Sensory reinforced corticostriatal plasticity

Nicolas Vautrelle[1,2†], Véronique Coizet[2,3†], Mariana Leriche[1,2], Lionel Dahan[2,4], Jan M. Schulz[1,5], Yan-Feng Zhang[1,6], Abdelhafid Zeghbib[2], Paul G. Overton[2], Enrico Bracci[2], Peter Redgrave[2] and John N.J. Reynolds[1 *]

[1] Department of Anatomy, Brain Health Research Centre, University of Otago, Dunedin 9054, New Zealand

[2] Department of Psychology, University of Sheffield, Sheffield, S10 2TP, UK

[3] Université Joseph Fourier, Inserm, U1216, Institut des Neurosciences de Grenoble, 38706 La Tronche Cedex, France

[4] Université de Toulouse, UPS, Centre de Recherches sur la Cognition Animale, 118 Route de Narbonne, F-31062 Toulouse Cedex 9, France

[5] Department of Biomedicine, University of Basel, CH - 4056 Basel, Switzerland

[6] Department of Clinical and Biomedical Sciences, University of Exeter Medical School, Hatherly Laboratories, Exeter EX4 4PS, United Kingdom

SUPPLEMENTARY FIGURES

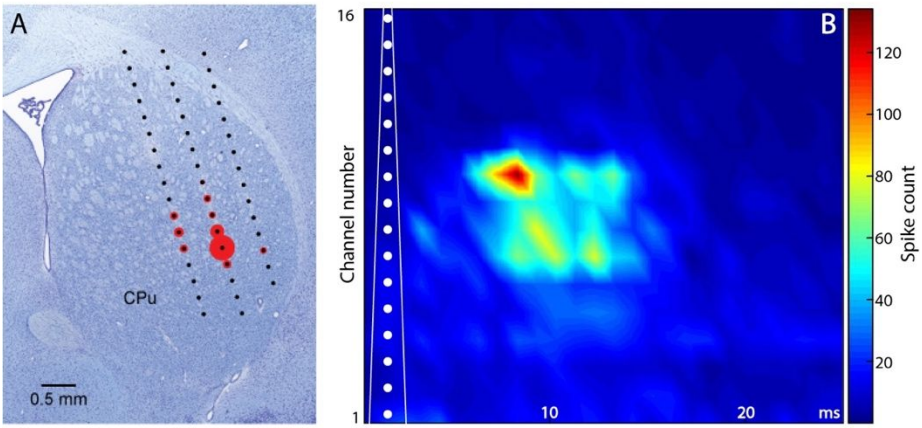

Fig. S1: Localized multi-unit responses evoked in the striatum by stimulation of motor cortex. **A.** An individual example of initial mapping used to establish the best location in the striatum for recording responses evoked by single pulse electrical stimulation of ipsilateral motor cortex. Responses were located in the lateral part of the striatum and extended approximately 1 mm in the rostro-caudal dimension. This information was used to guide probe placement in subsequent experiments. The size of red circles represents the relative magnitude of the evoked multi-unit response (see Fig 5). Abbreviation: CPu, caudate putamen. **B.** An individual example of peri-stimulus histogram obtained after processing striatal multi-unit responses to ipsilateral motor cortex stimulation recorded over 16 channels (120 stimulations/block).

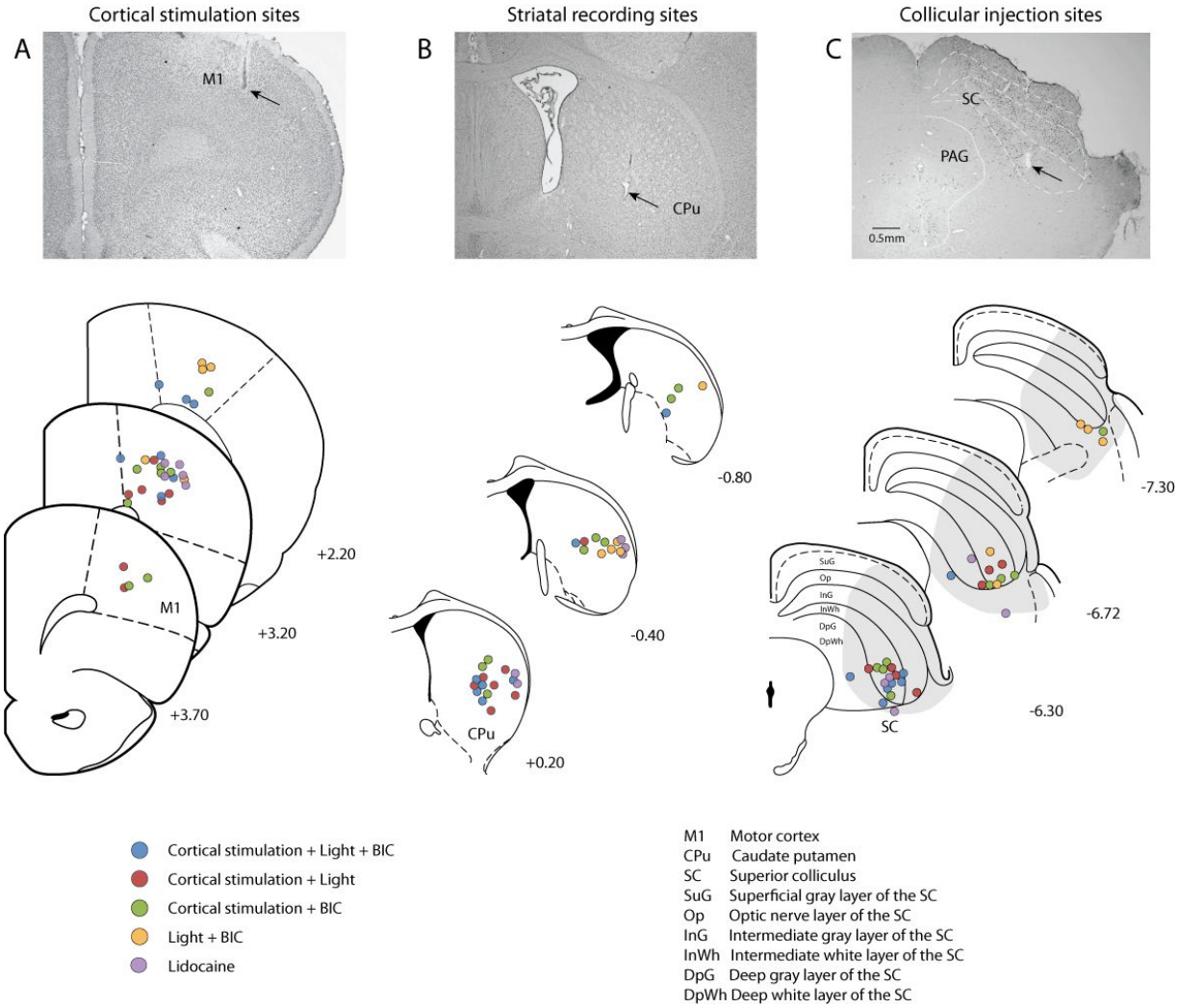

Fig S2: Reconstructions of stimulation, recording and injection sites from the first series of experiments. **A.** A photomicrograph of a typical stimulation site (arrow) in a section of motor cortex stained with cresyl-violet, and schematic representations of the stimulation sites for the different experimental conditions. **B.** A photomicrograph of a typical recording site (arrow) in a section of caudate putamen stained with cresyl-violet, and schematic representations of recording sites for the different experimental conditions. **C.** A photomicrograph of a typical injection site (arrow) in the superior colliculus and schematic representations of injection sites for the different experimental conditions. Note in the photomicrograph the distribution of neurons expressing Fos-like immunoreactivity in response to their activation by bicuculline and visual stimulation. A typical distribution of Fos-positive neurons following an injection of bicuculline into the superior colliculus is indicated by the grey shading in the schematic sections. The number associated with each section indicates mm relative to bregma.

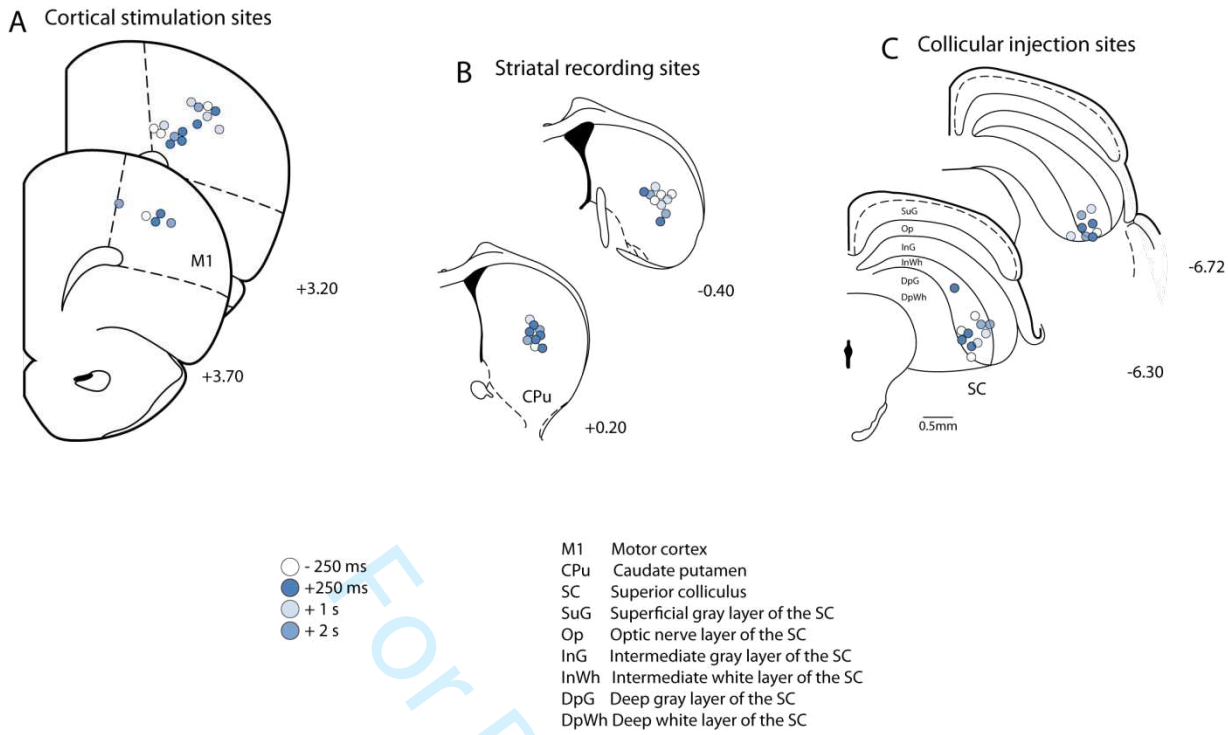

Fig S3: Reconstructions of stimulation, recording and injection sites from the second series of experiments. Schematic representations for the different experimental conditions of the stimulation sites in motor cortex **(A),** the striatal recording sites **(B)** and the collicular injection sites **(C).**

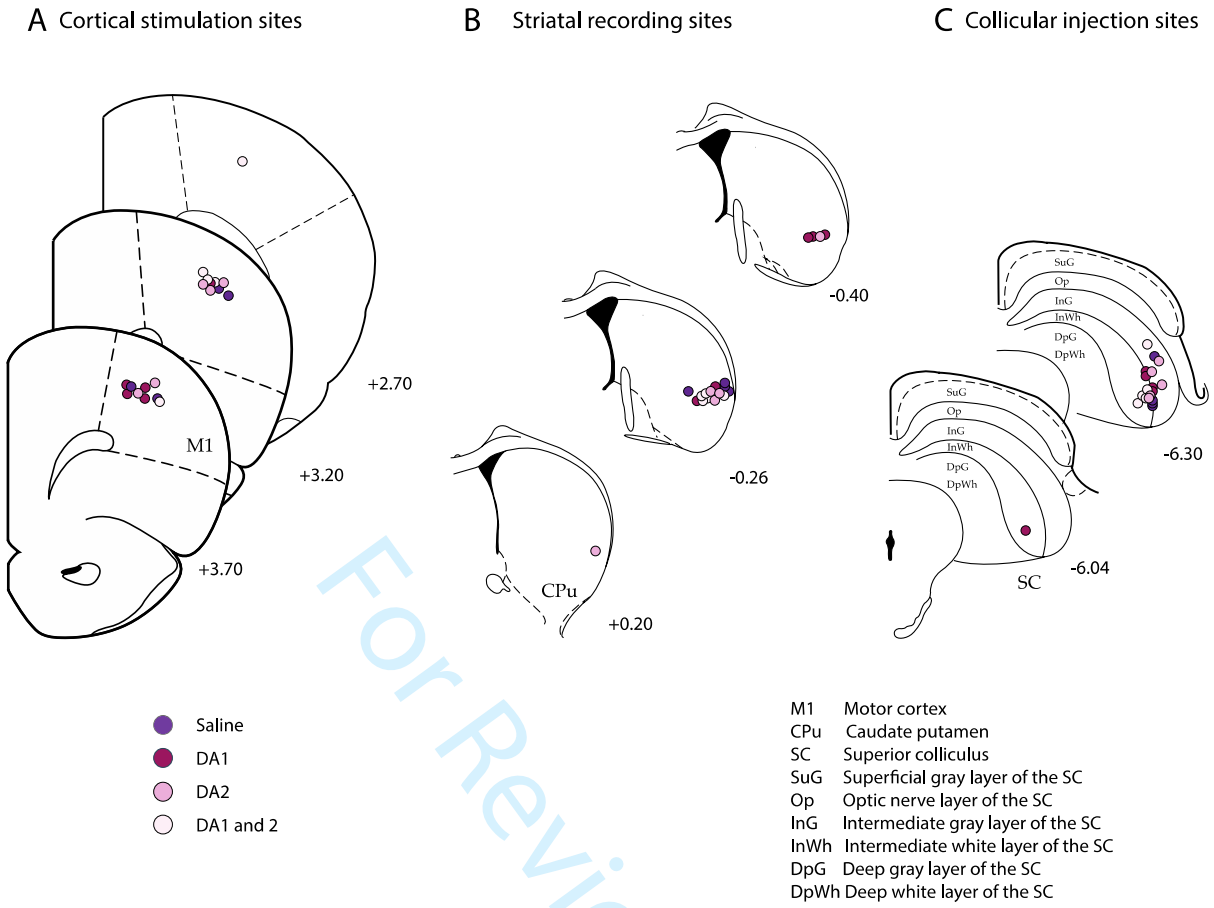

Fig S4: Reconstructions of stimulation, recording and injection sites from the third series of experiments. Schematic representations for the different experimental conditions of the stimulation sites in motor cortex **(A),** the striatal recording sites **(B)** and the collicular injection sites **(C).**

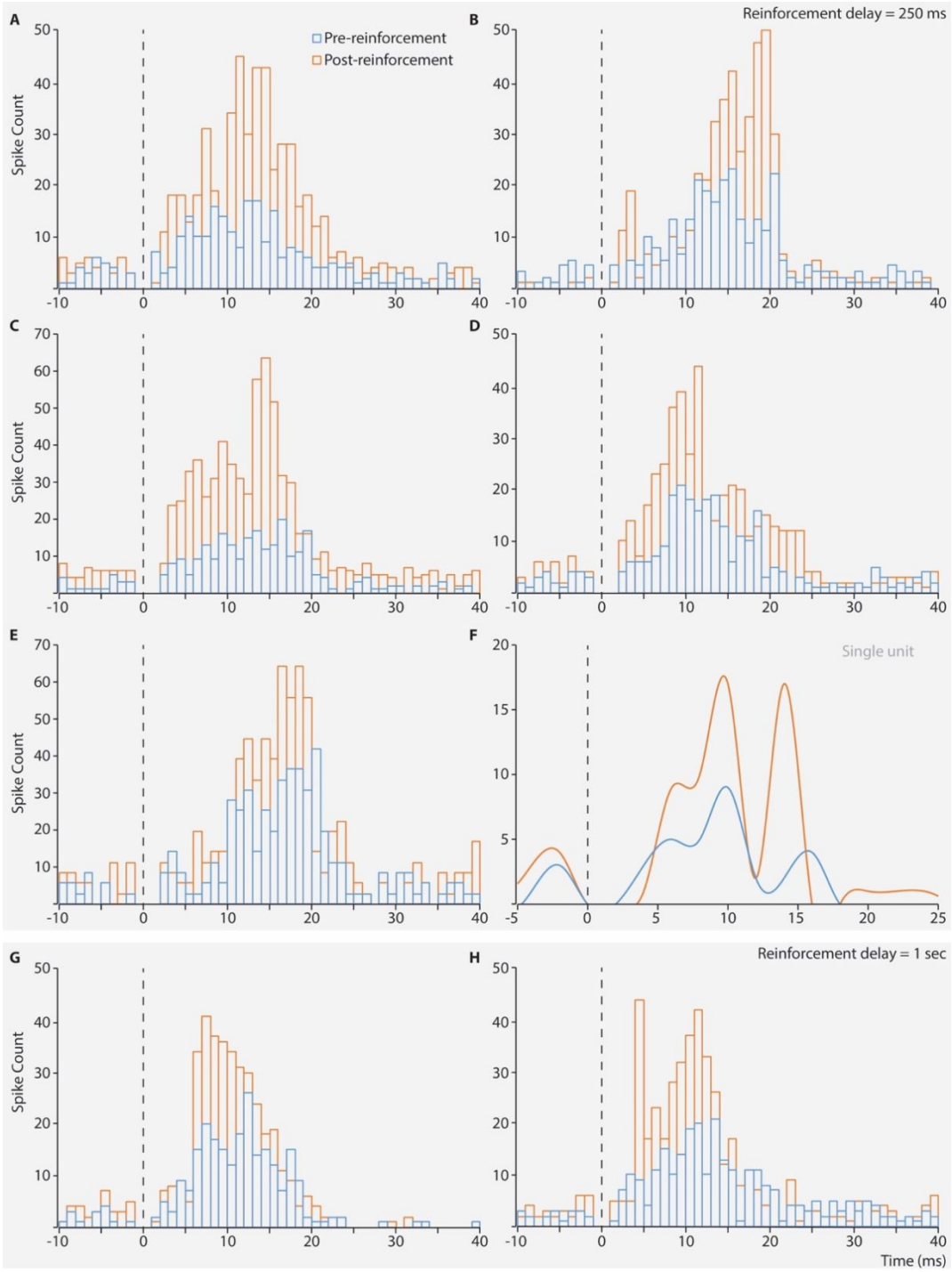

Fig. S5: Sensory-reinforced corticostriatal plasticity. **A-E.** Single case examples of striatal multi-unit potentiation induced by a delayed sensory reinforcer presented +250 ms after motor cortex stimulation. Comparison of peri-stimulus histograms obtained from pre-reinforcement and post-reinforcement recording blocks of 120 stimulations. **F.** Single case example of striatal single-unit potentiation induced by a delayed reinforcer presented +250 ms after motor cortex stimulation (60 stimulation blocks). **G-H.** Single case examples of striatal multi-unit potentiation induced by a delayed sensory reinforcer presented +1 sec after motor cortex stimulation (120 stimulation blocks).

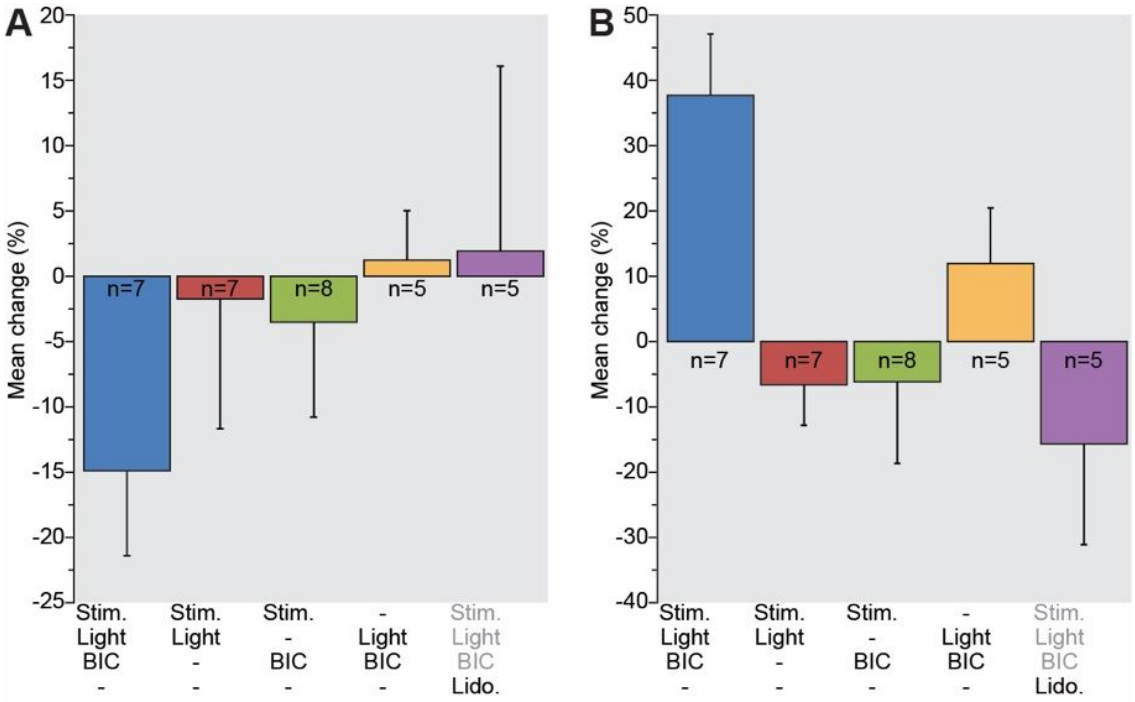

Fig. S6: Changes in corticostriatal response latency and duration. **A.** For all experimental conditions, mean change (%) in the latency of the cortical stimulus-evoked striatal responses 44-56min after collicular disinhibition (grey shaded area in Fig 2A). **B.** For all experimental conditions, mean change (%) in the duration of the cortical stimulus-evoked striatal responses 44-56min after collicular disinhibition. A significant increase in the duration of the striatal response accompanied the increase in response amplitude observed following collicular disinhibition.

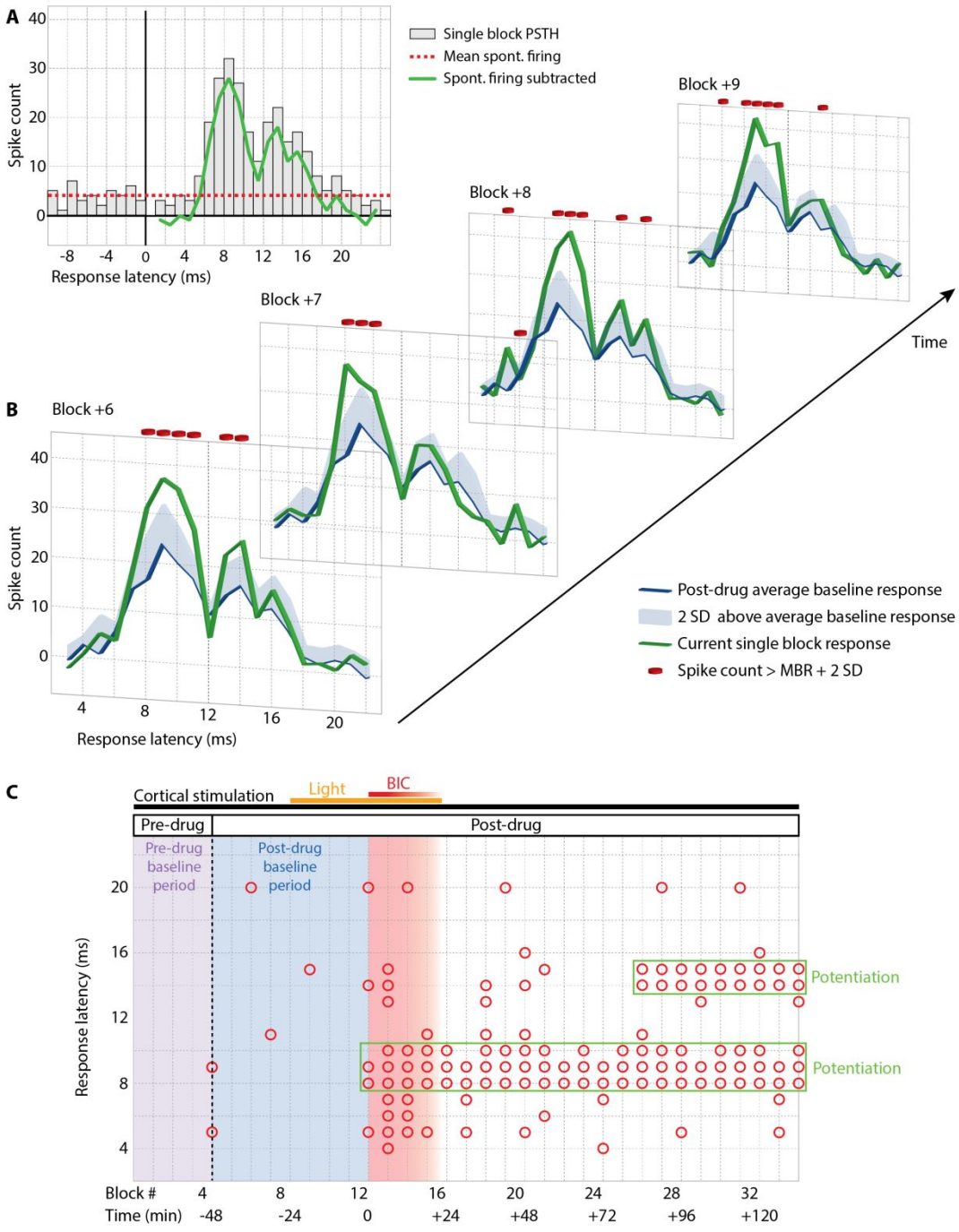

Fig. S7: Experimental protocol and data analysis of corticostriatal potentiation following the administration of dopamine antagonists. Striatal multi-unit responses to ipsilateral motor cortex stimulation were recorded simultaneously at different depths with a 16-channel electrode (NeiroNexus). This figure illustrates the classification of observed potentiation on a single channel following a period of sensory reinforcement (collicular disinhibition - BIC). **A.** Example of a single block (120 cortical stimulations) post-stimulus time histogram (grey bars) aligned to the cortical stimulus onset. For each PSTH, the absolute corticostriatal response (green line) was obtained by subtracting the mean pre-stimulus spontaneous firing (red dashed line) from the total response. **B.** Following the onset of sensory reinforcement (disinhibition of the superior colliculus with bicuculline) the

histograms of successive block responses (green lines) were compared to the post-drug average baseline histogram (blue lines); this was calculated for each channel over the 8 blocks preceding collicular disinhibition. If the spike count value of any 1ms bin of the single block response was greater than the sum of the spike count value + 2 standard deviations (blue shading) for the same bin of the average baseline response (blue line), this bin was considered to be potentiated (red circle). **C.** Example of consistent potentiation (red circles surrounded by green boxes) observed within an experimental session. Single cortical pulses (0.33Hz) were presented throughout (top black bar). Following a pre-drug baseline period (4 blocks of 120 stimulations – purple shading) and halfway through the post-drug baseline period (blue shading), cortical stimulation was paired with a light flash (+250ms – yellow bar). This light flash was ineffective at inducing potentiation until the SC was disinhibited by local injection of bicuculline (BIC - red bar and shading). Peaks of potentiation (open red circles; compare with B.) were plotted against time with respect to the injection of bicuculine (x axis) and the response latency to cortical stimulation (y axis). An overall striatal response was classified as potentiated (green boxes) if potentiation peaks with similar latencies were detected: i) over a minimum of 5 consecutive blocks; or ii) over 7 or more consecutive blocks and such peaks were absent during the post-drug baseline period.

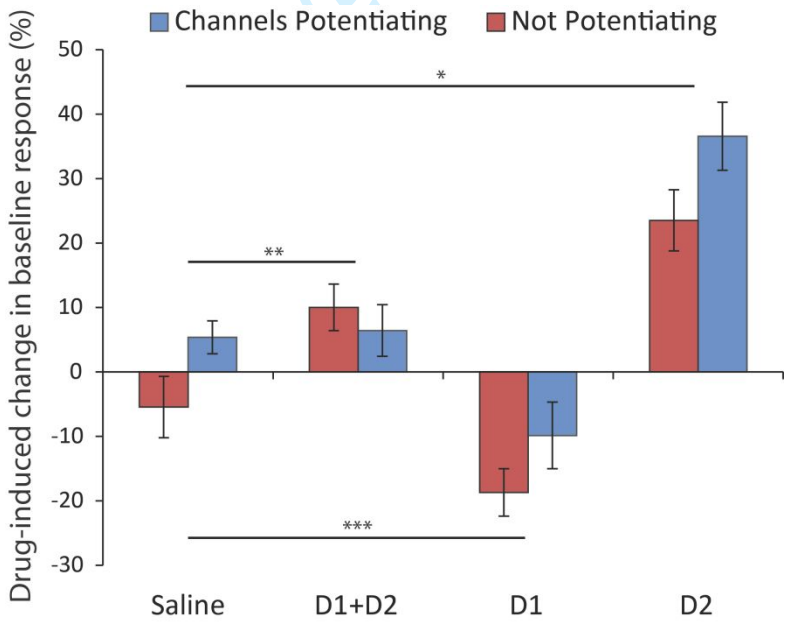

Fig. S8: Effect of DA antagonists on baseline striatal responses to cortical stimulation. Systemic administration of the D1-type receptor antagonist SCH23390 (0.2mg/kg) suppressed baseline striatal responding to the electrical stimulation of the motor cortex. Administration of the D2-type receptor antagonist sulpiride (30 mg/kg) enhanced the striatal response to cortical stimulation. When a combination of both antagonists was administered, a small but significant increase in the baseline striatal response was observed. In each condition, the effect of dopamine receptor antagonists on basal striatal responding did not differ between electrode channels that would later

potentiate or not (randomisation test based on the F statistic, D1type receptor blocker: F=28.55, $P = 0.0001$; D2 receptor blocker: F=4.81, $P = 0.0321$; D1+D2 type receptor blockers: F=9.71, $P = 0.0015$).